T-1133

A STUDY OF THE THERMAL CONDUCTIVITY AND THERMAL DIFFUSIVITY OF SANDSTONE RESERVOIR ROCKS UNDER A VACUUM

1969

BY

HOMER J. BOYD

ProQuest LLC.
789 East Eisenhower Parkway
P.O. Box 1346
Ann Arbor, MI 48106 – 1346

T-1133

A thesis submitted to the Faculty and the Board of Trustees of the Colorado School of Mines in partial fulfillment of the requirements for the degree of Master of Science in Petroleum Engineering.

Signed: Homer J. Boyd
Homer J. Boyd

Approved: D. M. Bass
Prof. D. M. Bass
Thesis Advisor

D. M. Bass
Prof. D. M. Bass
Head, Department of
Petroleum Engineering

ABSTRACT

Investigations were made to determine the thermal conductivity (k) and thermal diffusivity (H) of porous arkosic sandstones. These thermal properties were determined and illustrated as functions of temperature, porosity, and permeability. Correlations were obtained between the thermal properties and porosity.

The tests were conducted under a pressure of less than 10 microns and a temperature range of 70° F. to 600° F. Time and temperature at pre-selected stations were the parameters measured during an experimental run.

Two standard materials, Coors' porcelain AD-85 and a satin surface quartz rod, were subjected to the same experimental procedure as were sandstone specimens to establish a check on the results obtained.

This experimental work was performed to determine k and H of a porous rock in the absence of a saturating fluid, to establish an effective and relatively easy procedure for determining the thermal properties (k, H) of a porous medium under a vacuum, and to determine if a correlation between thermal and physical properties of the sandstone existed.

The results of this work proved that the experimental procedure was an effective way for determining the above mentioned thermal properties. A correlation between the thermal properties and porosity has been shown to exist. The correlation of thermal properties with permeability is, however, dependent upon a correlation between permeability and porosity (Figure 53).

Included in the appendix are two IBM 360 computer programs written in Fortran IV language, a derivation of the equations used for the experimental procedure, geological description of specimens, sample heating and cooling curves, equations for steady-state surface temperature profiles, and a tabulation of porosity, permeability, bulk density, thermal conductivity and thermal diffusivity.

CONTENTS

T-1133

ACKNOWLEDGEMENTS

The author wishes to thank Professor D. M. Bass for serving as thesis advisor, suggesting this research project, and giving encouragement toward the completion of this project.

The author wishes to express appreciation to several other people who have contributed to this work. Some of the people to whom the writer is indebted are: Mr. Lee Richardson, Mr. R. I. Meyer and Mr. Max Stone of Atlantic Richfield's Research Laboratory in Bakersfield, California; the Atlantic Richfield Company, which financed the major portion of this research project; Dr. Charles Bouchillion and Mr. Percy Payne of Mississippi State University for several hours of discussion on the mechanics of heat transfer.

Finally, the author expresses thanks to those who have served as thesis committee members: Professors John D. Haun, Jerry Bergeson, and P. F. Dickson.

INTRODUCTION

During the past decade the possibility of oil recovery through thermal stimulation became an economic reality. Prior to 1950 two insitu combustion test projects were initiated in the Childress and Southern Oklahoma fields near Oklahoma City. In 1956 a major oil company began field experiments with steam injection in the Coalinga area of California. At about the same time, another major company started an insitu combustion project in Illinois.

Since 1956 the interest in thermal stimulation as an oil recovery technique has continued to increase. This increased interest is confirmed by the initiation of thermal recovery projects in the San Juaquin Valley, Ventura Basin, and Los Angeles Basin of California, in addition to areas of Texas, Illinois, Indiana, and South America.

The initiation of any thermal stimulation process raises several problems. For steam injection projects, the heat loss from surface to the hydrocarbon-bearing formation must be evaluated, as must the heat loss to adjacent formations. Insitu combustion processes are concerned primarily with the heat loss to adjacent formations. Regardless of the thermal stimulation process used, an estimate of the effectiveness of the heat within the hydrocarbon-bearing formation

must be made, i. e., for a given amount of heat input, how much rock and fluid will be heated and to what temperature?

It is obvious at this point that thermal properties of the solid and fluid within the porous medium must be known to make the necessary calculations. A survey of the literature revealed no information on the thermal properties of the solid part of the porous medium, thus the primary prupose of this investigation.

Thermal conductivity has been the subject of many research projects, the majority of which have little application to the evaluation of thermal oil recovery processes. A large portion of the published work consists of the determination of thermal conductivity of materials with different chemical composition and geometrical shapes (5, 8, 9, 17).

Birch and Clark (3) were two of the earlier investigators of the thermal properties of rocks. These writers illustrated the dependency of thermal conductivity upon temperature and chemical composition. Several rock samples (igneous and sedimentary) were subjected to temperatures ranging from 0° C. to 500° C. at atmospheric pressure.

Zierfuss and van der Vliet (26) made a significant contribution with their work on thermal conductivity in sedimentary rocks. Fifty samples of different composition, permeability, porosity, and formation resistivity (FRF) were subjected

to temperatures of 0° C. to 300° C. at atmospheric pressure in the presence of a saturating fluid. The results of their studies showed the effect of using various saturating fluids upon the thermal conductivity of the rock-fluid system. The effects of chemical composition of the rock upon thermal conductivity was illustrated. The product of FRF and porosity suggested a correlation with thermal conductivity.

Somerton (21) was one of the first to conduct research on the thermal properties of sedimentary rocks with the purpose of obtaining data used in thermal oil recovery calculations. In this work, ten samples of sandstone, silty sand, siltstone and/or shale were subjected to temperatures ranging from 90° F. to 980° F. These experiments were conducted with the specimens saturated with fluids of known thermal properties at pressures of 14.7, 500, 1500, or 3000 psia. The results of Somerton's work showed the dependency of heat capacity (cp), thermal conductivity (k), and diffusivity (H) upon temperature and pressure.

The determination of thermal diffusivity was the main objective of Somerton and Boozer's (22) research. Samples of sandstone were subjected to temperatures ranging from 200° F. to 1800° F. in the presence of a saturating fluid at atmospheric pressure. The results of this research showed the dependency of thermal diffusivity, conductivity, and heat capacity upon temperature.

The previously discussed literature dealt with the thermal properties of rocks filled with a saturating fluid. Schotte (19) showed the influence of the presence of a saturating fluid (gas) on the laboratory measured thermal properties. Kunii and Smith (15) also studied the thermal conductivity of sandstone samples saturated with a fluid. This latter work was the basis for another publication by Kunii and Smith (16) in which the thermal conductivity of the saturated sample was measured. This research was performed at pressures of 0.039 to 400 psia. The samples were saturated with either n-heptane, methyl alcohol, water, or a water-glycerol solution. Measurements were taken with the saturated specimen in a gas environment of helium, nitrogen, air, or carbon dioxide. The permeability of the samples ranged from 18 to 590 md.

The results of this work were used to evaluate a theoretical equation developed earlier (15) to predict the thermal conductivity of a rock filled with a fluid of known thermal properties.

The equation developed in (15) and evaluated in (16) is

$$\frac{K_e^\circ}{K_s} = \phi'\left(\frac{K_g}{K_s}\right) + \frac{(1-\phi')\left(1+\frac{\phi'}{\phi}\alpha\right)}{1+\frac{\phi'/\phi}{\frac{1}{\alpha}\left(\frac{K_g}{K_s}\right)+\frac{D_p H_p}{K_s}}}.$$

in which k_e°, k_s, and k_g are the thermal conductivity of the saturated specimen, solid portion of the rock only, and the gas environment, respectively. ϕ is the porosity of the unconsolidated packed beds, and ϕ' the porosity of sandstone.

Prior to evaluating the above equation, k_s must be determined. As far as the writer has been able to determine, no direct determinations of thermal conductivity and diffusivity of a porous rock in the absence of a saturating fluid have been made. A portion of the literature surveyed illustrates the effect of a saturating fluid upon the heat conduction through a porous medium. The equations developed for the determinations of k and H in a saturated porous medium require the thermal conductivity of the solid portion of the rock.

The following data were presented (16) to show the effect of a saturating fluid upon thermal conductivity and to illustrate the importance of being able to determine the thermal conductivity of the solid portion of the rock.

k_e°	k_s
4.40 BTU/ft^2/In/Min/$^\circ$R	9.40 BTU/ft^2/In/Min/$^\circ$R
3.45 BTU/ft^2/In/Min/$^\circ$R	18.10 BTU/ft^2/In/Min/$^\circ$R
4.05 BTU/ft^2/In/Min/$^\circ$R	23.00 BTU/ft^2/In/Min/$^\circ$R
6.10 BTU/ft^2/In/Min/$^\circ$R	20.00 BTU/ft^2/In/Min/$^\circ$R

where k_e° and k_s are as previously defined.

EXPERIMENTAL PROCEDURE

Twenty-six sandstone specimens, one inch in diameter, from the Stevens, Refugain, and Eocene sands of California were selected for this research on the basis that the specimens represent an acceptable range of porosity (5-30%) and permeability (0-300 md). Prior to experimentation each specimen was indexed at lengths of 1, 1-1½, or 2 centimeters. The specimens were then placed into an oven, heated to above 400° F. for a minimum for two days, and placed in a desicator for storage.

Thermocouples were placed on the exterior and the heat source attached to one end of the prepared specimen prior to insertion into the vacuum chamber (see Figure 1).

The heat source was generated by applying a constant current of one, two, or three amps to sixteen gage nichrome wire which was wound around, but electrically insulated from, the copper heating element.

Two separate but similar set-ups were used to obtain the reported data. All sandstone specimen were run using a sixteen point recorder while the standard materials were run utilizing a twenty-four point recorder. All other components of the experimental equipment were identical.

Table I gives heating element wire data and energy inputs for the three heating elements used during this research. Also presented are pertinent data on the two standard materials used.

An experimental run was accomplished according to the following steps:

1. Determination of heat capacity as a function of temperature;
2. Positioning of the specimen inside the plexiglas vacuum chamber;
3. Evacuation of the vacuum chamber to less than 10 microns pressure;
4. Application of the current to the heat source and monitoring of the surface temperature with a 16 or 24 point recorder (galvanometer) using Chromel - alumel thermocouples;
5. Maintaining of heat source until the temperature along the specimen has reached a steady-state, i.e., the temperature at any point ceases to increase;
6. Shutting off of power to heating element and monitoring temperature profile for several minutes;
7. Evaluation of the equation

$$D/K = f(T_{aa}) = \frac{A\left(\frac{dt}{dx}\Big|_{x2} - \frac{dt}{dx}\Big|_{x1}\right)}{\sigma A_s \left(T_{aa}^4 - T_s^4\right)}$$

8. Plotting D/k as a function of temperature (T_{aa}) is used to exclude that portion of the curve that exhibits end effects;

9. Using $f(T_{aa})$ as determined in (7) to evaluate

$$K = \frac{Mc_p(T_{a\theta 2} - T_{a\theta 1})/\Delta\theta}{A\left(\frac{\partial t}{\partial x}\Big|_{x2} - \frac{\partial t}{\partial x}\Big|_{x1}\right) - \sigma A_s f(T_{aac})(T_{aac}^4 - T_s^4)}$$

by using program "Thermal Conductivity Coeff Calculation";

10. Calculation of thermal diffusivity by the following equation:

$$H = K/c_p\rho$$

A derivation of the equations in Step 7 and 9 are included in the appendix. Also presented is an alternate method for determining H from the transient data.

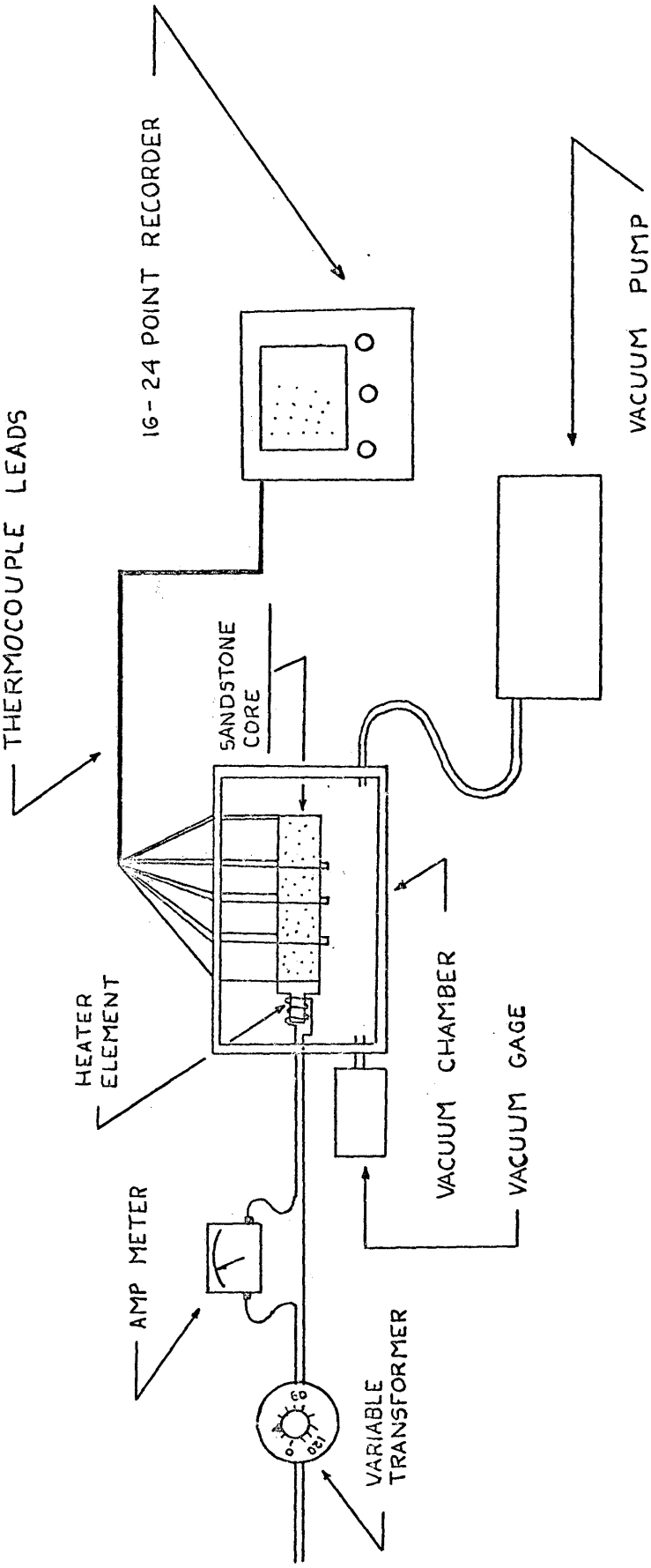

FIGURE 1 LABORATORY EQUIPMENT SET-UP

TABLE 1

HEATING ELEMENT DATA

HEATER	WIRE LENGTH	TYPE WIRE	RESISTANCE
1	37"	Nichrome 16 gage	1.8 ohms/ft.
2	33"	Nichrome 16 gage	1.8 ohms/ft.
3	29"	Chromel 16 gage	1.04 ohms/ft.

ENERGY INPUT TO HEATER ELEMENT

HEATER	INPUT CURRENT	WATTS	BTU/MIN
1	1 amp.	5.40	0.307
	2 "	21.60	1.229
	3 "	48.60	2.764
2	1 "	4.95	0.282
	2 "	19.80	1.126
	3 "	44.55	2.534
3	1 "	2.51	0.143

TABLE 1 - - ENERGY INPUT TO HEATER ELEMENT (Continued)

Heater	Input Current	Watts	BTU/MIN
3	2 amp	10.04	0.571
	3 "	22.59	1.285

THERMAL PROPERTIES OF STANDARD MATERIALS

(Coors Porcelain AD-85)

C_p @ 672°R	Diameter	k
0.22 BTU/lbm-°R	1.06 inches	1.691 BTU/in/ft^2/min/°R @ 528°R
		1.403 " " " @ 672°R
		0.774 " " " @1212°R

(Satin Surface Quartz Rod)

C_p @ 672°R	Diameter	k
0.219 BTU/lbm-°R	1.00 inches	1.596 BTU/in/ft^2/min/°R @ 672°R

DISCUSSION OF RESULTS

Steady-state surface temperature profiles for the test specimens from which the radiation-conduction ratio, D/k, was determined are plotted on Figures 7 through 36. Evaluation of any of the equations (Table 2) of the measured steady-state temperature profiles indicates that the temperature profiles can be represented by a second order equation, thereby satisfying one of the restrictions placed on the use of equation (5a) of the appendix.

D/k was presented graphically as a function of temperature in Figure 37. The graph shows that as the temperature increases, the D/k factor decreases. The inverse proportionality between D/k and temperature was expected due to the change in the denominator with respect to T_{aa} of equation (1b) of the appendix.

Figures 39 through 48 illustrate the dependency of thermal conductivity and diffusivity upon temperature. This phenomenon was expected and has been published by several authors (21). It is interesting to note that above about 200° F. the thermal properties cease to change significantly with additional increases in temperature.

A correlation between thermal conductivity and diffusivity exists with porosity as is illustrated by Figures 49 and 50.

The correlation of these two thermal properties with porosity is explained by examining torturosity as a function of porosity.

In this research the thermal conductivity has been defined as

$$K = A\Delta T/\Delta X \tag{1}$$

in which $A = \pi d^2/4$ and ΔX is the straight line distance over which ΔT occurs, however, the thermal conductivity of the solid portion of the rock, k_r, is

$$K_r = \frac{A(1-\phi)\Delta T}{\Delta X(\tau)} \tag{2}$$

in which $1-\phi$ compensates for the reduction of cross-sectional area due to porosity and τ, the tortuosity, accounts for the additional length in the flow path due to porosity.

Now,

$$\frac{K_r}{K} = \frac{\frac{A(1-\phi)\Delta T}{\Delta X(\tau)}}{\frac{A\Delta T}{\Delta X}} = \frac{1-\phi}{(\tau)} \tag{3}$$

then $$K = \frac{K_r(\tau)}{(1-\phi)} \tag{3a}$$

Figure 2 illustrates how the measured thermal conductivity will vary as a function of tortuosity, thus as a function of

porosity. Using boundary conditions of $\phi = 0$, $\tau = 1-\phi$, $\tau = 1$, or τ = non-linear function of porosity will establish the following curves.

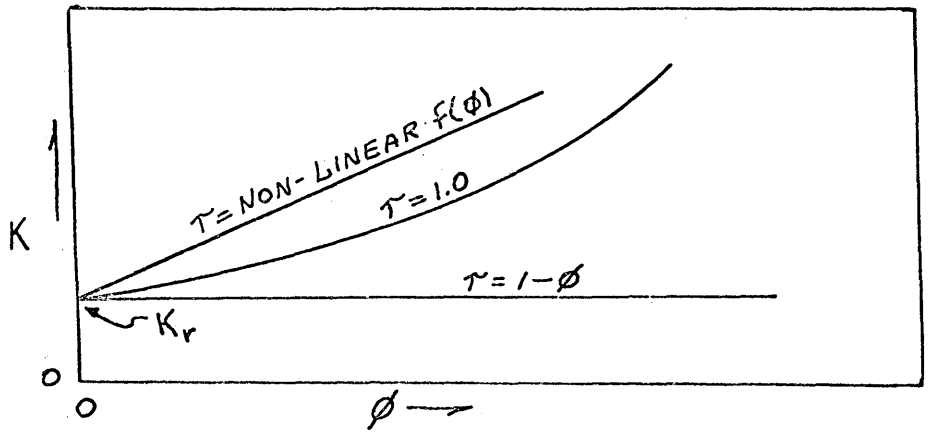

Figure 2. Measured k as a function of porosity.

From equation (3a) it is evident that when porosity (ϕ) is zero $k = k_r\tau$. It is further noted that when $\tau = 1 - \phi$, the thermal conductivity (k) of the porous medium is independent of porosity. If the tortuosity (τ) is unity then k would approach infinity as the porosity approaches unity. Finally if τ is some non-linear function of porosity, k will increase at some constant rate with respect to porosity or

$$k = k_r + m\phi \tag{4}$$

in which m is the slope of the straight line.

Substituting equation (3a) in equation (4) gives

$$K_r\tau/(1.-\phi) = K_r + m\phi \tag{5}$$

Solving for τ yields

$$\tau = (1+m\phi/K_r)(1-\phi) = 1+(m/K_r-1)\phi - m\phi^2/K_r \tag{6}$$

Using equation (6) in (3a) gives

$$K = K_r \gamma/(1-\phi) = K_r[1+(m/K_r - 1)\phi - (m/K_r)\phi^2]/(1-\phi) \qquad (7)$$

$$= [K_r + (m - K_r)\phi - m\phi^2]/(1-\phi)$$

which establishes the correlation of thermal conductivity with porosity.

Specimens S-3, S-4, and S-7 display a slightly higher value of k than does S-1A, S-2A, S-8, and S-9. The difference in k of these two sets of specimens is natural owing to the cementing material of the specimens. S-3, S-4, and S-7 are cemented with calcite while the other specimens are cemented primarily with montmorillonite. The effect of chemical composition on thermal conductivity and diffusivity has been previously illustrated (21, 22).

Figure 53 shows the relationship between permeability and porosity for the specimens used in this work.

The thermal conductivity measured for the standard materials was plotted as a function of temperature and is presented on Figures 39 and 40. Comparison of the measured values of thermal conductivity with the published data indicates a discrepancy of about 40% at 200° F. The same comparison at 100° F. indicates better agreement between the two values, or about 30%

disagreement. Better agreement at lower temperatures was expected because the measured temperature more closely approached the true surface temperature of the specimen.

The discrepancy exists for three reasons:

1. The center-line temperature was not used in the determination of k;
2. Thermocouples were not uniformly attached to the specimens;
3. Bare thermocouple wire was permitted near the thermocouple junction, allowing heat loss from the wire by radiation.

Figure 3 shows variations in temperature measurements obtained due to different methods used to attach thermocouples to the surface of an iron pipe.

The following example illustrates the effect of using surface temperature measurement as opposed to center-line temperature.

Let $T = 189.0 - 35.4X - 3.02X^2$

then $dt/dx = - 35.4 - 6.04X$

The surface temperature at X = 1 and X = 2 is 156° F. and 130° F. for a ΔT of 26 degrees. Using dt/dx at X = 1 and X = 2 gives center-line temperatures of 185.8 and 153.7 for a ΔT of 32.1. The discrepancy between the measures thermal conductivity k and actual thermal conductivity k_a due to using surface temperatures will be $K = (K_a)(26/32)$

Of the data in the literature, none are appropriate for comparison with the results obtained in this research. Kunii and Smith (16) reported thermal conductivity for the solid material of a packed bed, however, the temperature at which k was measured was not given.

FIGURE 3

Comparison of Methods of Attaching Thermocouples to the Surface of an Iron Pipe.

1. Peened into hole in rust covered surface.
2. Peened into hole in brazed-over surface.
3. Brazed to surface.
4. Brazed to surface - thermocouple wire wrapped around pipe once.
5. In an oil filled hole in rust covered surface.
6. Peened into hole in rust covered surface.

All thermocouple brazed junction, copper-constantan #24 wire.

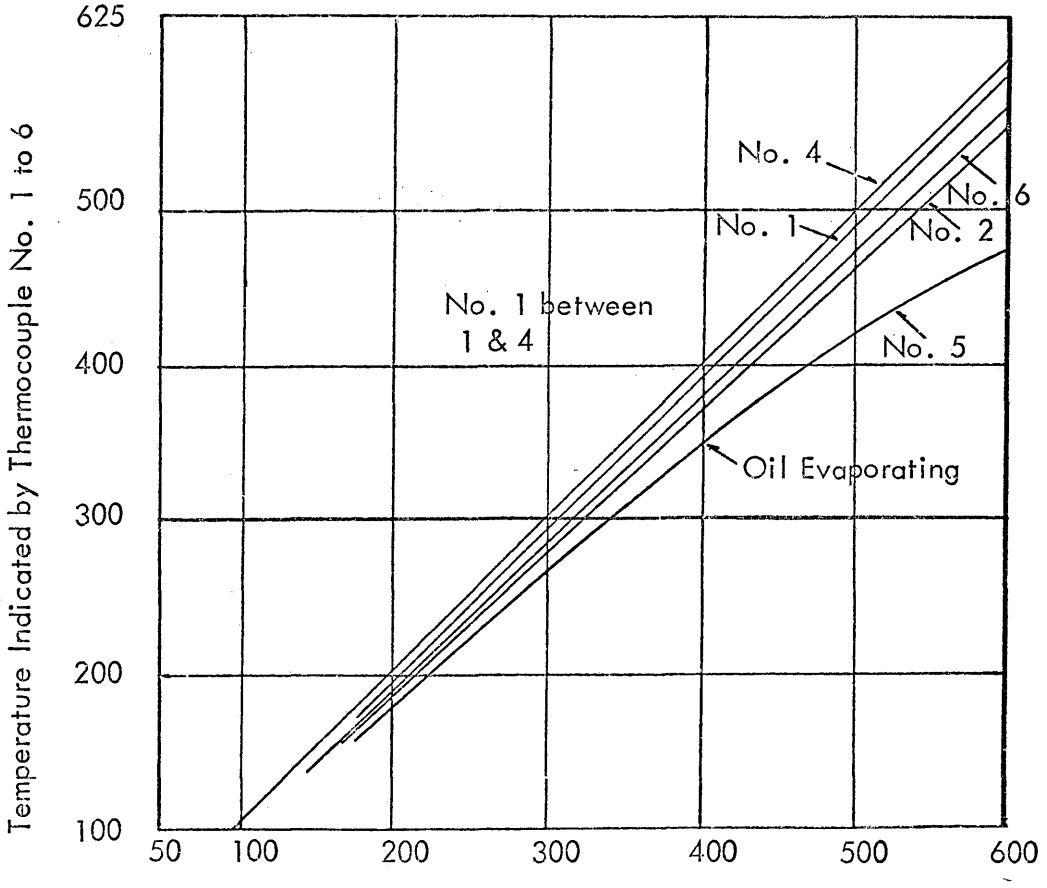

CONCLUSIONS

1. The experimental procedure used in this study is an effective way to determine thermal conductivity and thermal diffusivity.

2. A correlation between thermal conductivity and porosity does exist and has been established.

3. Thermal conductivity and thermal diffusivity of arkosic sandstones become relatively small at temperatures in excess of 200° F.

4. Additional work should be done in this area on other sedimentary rocks.

RECOMMENDATIONS

1. Obtain a pressure of 10 microns or less inside the vacuum chamber to render heat loss by convection negligible.
2. Calibrate the temperature recorder over the expected operating temperature range.
3. Insure good thermal contact between heater element and specimen.
4. Attach thermocouples uniformly to specimen and cement into position.
5. Wrap thermocouples around the specimens about two times, following an isothermal plane.

APPENDIX

DERIVATION OF THE ONE DIMENSIONAL STEADY-STATE AND TRANSIENT HEAT CONDUCTION EQUATION

Before the specific problem at hand is discussed the differential equation governing the temperature distribution in a body will first be derived; then by making certain symplifying assumptions the equation will be reduced into a form applicable for analytical, graphical, or numerical solutions.

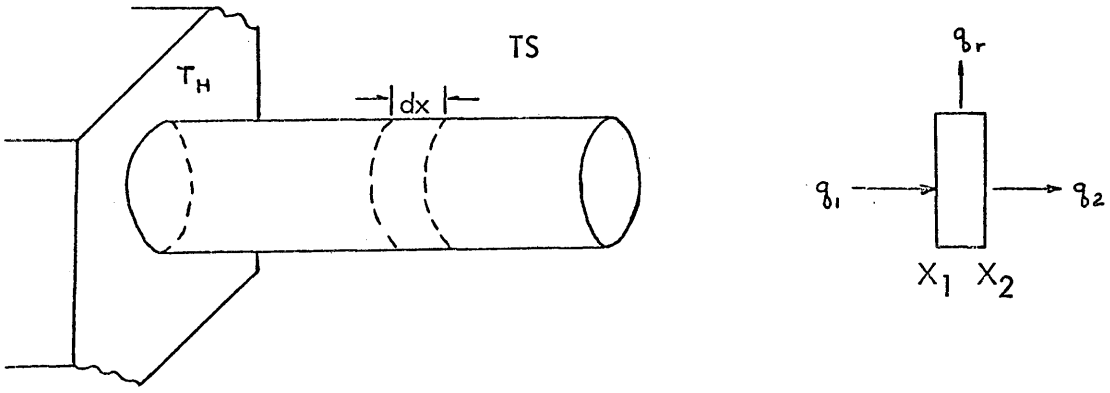

Figure 4. Sketch and nomenclature for a rod protruding from a constant heat source.

Assume a rod to have constant cross-sectional area, surface area, specific heat, and assume that the conductivity k, diffusivity H and the emissivity e, are constant over small differences in temperature. Suppose the rod lies along

the X axis and consider the element of volume bounded by X_1 and X_2 (Figure 4a).

Under steady-state conditions the rate of heat flow into the element must equal the rate of heat flow out of the element, or:

Rate of heat flow by conduction into the element at X_1	=	Rate of heat flow by conduction out of the element at X_2	+	Rate of heat flow by radiation from the surface between X_1 and X_2

Symbolically the equation becomes:

$$-KA\frac{dt}{dx}\Big|_{X1} = -KA\frac{dt}{dx}\Big|_{X2} + \sigma FeA_s(T_{aa}^4 - T_s^4) \qquad (1)$$

Rearranging and solving for unknown quantities gives:

$$KA\left(\frac{dt}{dx}\Big|_{X2} - \frac{dt}{dx}\Big|_{X1}\right) = \sigma FeA_s(T_{aa}^4 - T_s^4) \qquad (1a)$$

thus

$$Fe/K = \frac{A\left(\frac{dt}{dx}\Big|_{X2} - \frac{dt}{dx}\Big|_{X1}\right)}{\sigma A_s(T_{aa}^4 - T_s^4)} \qquad (1b)$$

where F = shape factor
e = emissivity coefficient
σ = 2.868×10^{-11} BTU/min - ft^2°R (Stefan-Boltzmann/Constant.)
A = cross-sectional area of rod
As = surface area of rod between X_1 and X_2
T_{aa} = effective radiating surface temperature between X_1 and X_2 and defined mathmatically as

$$T_{aa} = \left(\frac{T_{x1}^4 + T_{x2}^4}{2.0}\right)^{0.25}$$

(From Steady-State Temperature)

T_s = temperature of the medium into which the heat is radiating (plexiglas vacuum chamber).

This, however, leaves three unknowns in one equation. It would be possible to set Fe = D and solve the equations simultaneously; however, since k is in fact a function of temperature, uniqueness of the solution would not be guaranteed. A solution can be obtained, however, in the following manner if cooling curves are available.

Consider the following temperature distribution curves for steady-state and cooling environments.

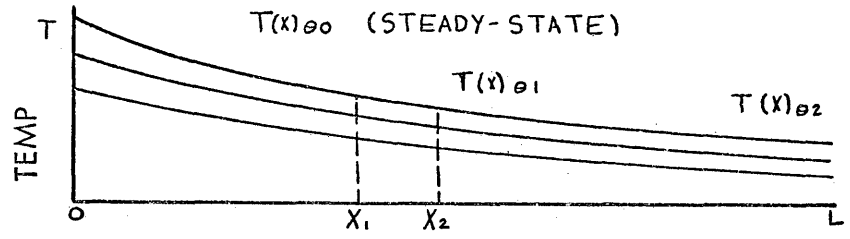

Figure 5. Temperature profiles along a rod.

Again considering the elemental volume bounded by X_1 and X_2, the change in internal energy can be expressed as:

$$\Delta U = U_{\theta 2} - U_{\theta 1} = mc_p(T_{a\theta 2} - T_{a\theta 1}) \tag{2}$$

Which must also equal the heat flow into the element less the heat loss from the element, or:

$$\Delta U = q_{b1} - q_{b2} - q_{b3} \tag{3}$$

Substitution of equation 1 into 3 gives:

$$\Delta U = \left[-KA\frac{\partial t}{dX}\Big|_{X1} + KA\frac{\partial t}{dX}\Big|_{X2} - \sigma DA_s\left(T_{adc}^4 - T_s^4\right)\right]\Delta\theta \tag{3a}$$

Now substituting equation 3a into equation 2 gives:

$$m c_p (T_{a\theta_2} - T_{a\theta_1})/\Delta\theta = KA\left(\frac{dt}{dx}\Big|_{x2} - \frac{dt}{dx}\Big|_{x1}\right) - \sigma D A_s (T_{aac}^4 - T_s^4) \qquad (4)$$

now from equation 1b let $f(T_{aa})$ equal

$$\frac{A\left(\frac{dt}{dx}\Big|_{x2} - \frac{dt}{dx}\Big|_{x1}\right)}{\sigma A_s (T_{aa}^4 - T_s^4)} \qquad (1c)$$

then

$$D = K f(T_{aa}) \qquad (1d)$$

substituting equation 1d into equation 4 gives:

$$m c_p (T_{a\theta_2} - T_{a\theta_1})/\Delta\theta = K\left[A\left(\frac{dt}{dx}\Big|_{x2} - \frac{dt}{dx}\Big|_{x1}\right) - \sigma A_s f(T_{aa})(T_{aac}^4 - T_s^4)\right] \qquad (5)$$

Rearranging equation 5 and solving for k yields:

$$K = \frac{m c_p (T_{a\theta_2} - T_{a\theta_1})/\Delta\theta}{A\left(\frac{dt}{dx}\Big|_{x2} - \frac{dt}{dx}\Big|_{x1}\right) - \sigma A_s f(T_{aa})(T_{aac}^4 - T_s^4)} \qquad (5a)$$

Thus, thermal conductivity is expressed as a function of the temperature T_{aac}. Particular caution must be applied in obtaining the various numerical values for substitution into the above equation; thus the following explanations:

m = mass of elemental volume (lbm)
Cp = specific heat (BTU/lbm-^{o}R)
$T_{a\theta 2}$ = average temperature between X_1 and X_2 at time two or

$$T_{a\theta_2} = (T_{x1,\theta_2} + T_{x2,\theta_2})/2.0$$

$T_{a\theta 1}$ = same as $T_{a\theta 2}$ except for time one (^{o}R)

$\Delta\theta$ = time two less time one (min)
A = cross-sectional area of rod (ft^2)
A_s = surface area between X_1 and X_2 (ft^2)
σ = as previously defined

$\left.\frac{dt}{dX}\right|_{xn}$ = average rate of change in temperature

with respect to length and is obtained algebraically as:

$$\left.\frac{\overset{\circ}{dt}}{dX}\right|_{xn} = \left(\left.\frac{dt}{dX}\right|_{xn,\theta i} - \left.\frac{dt}{dX}\right|_{xn,\theta i+1}\right) / 2.0$$

T_{aac} = average effective radiating temperature while specimen is cooling

$$= \frac{\left(\frac{T^4_{xn,\theta i} + T^4_{xn+1,\theta i}}{2.0}\right)^{0.25} + \left(\frac{T^4_{xn,\theta i+1} + T^4_{xn+1,\theta i+1}}{2.0}\right)^{0.25}}{2.0}$$

$f(T_{aac})$ = as defined previously but evaluated at T_{aac} $^{o}R/in$

DERIVATION OF THE UNSTEADY-STATE THREE DIMENSIONAL HEAT CONDUCTION EQUATION

In order to obtain an expression for thermal diffusivity, H, it will be necessary to expand the one dimensional steady-state heat flow equation into a three dimensional unsteady-state condition, thus resulting in an equation for the temperature distribution within the rod.

Consider a small rectangular elemental volume of material in a solid body as shown in Figure 6.

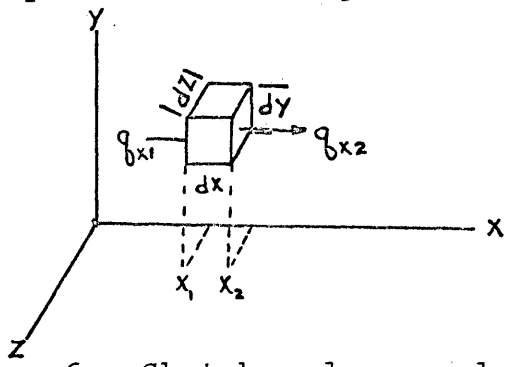

Figure 6. Sketch and nomenclature for three-dimensional heat flow.

The energy balance for the elemental volume during time $d\theta$ may be expressed as:

Heat flow into element during $d\theta$	+ Heat generated within element by internal source during $d\theta$	= Heat flow out of element during $d\theta$	+ Change in internal energy of element during $d\theta$

or

$$(q_{x1} + q_{y1} + q_{z1})d\theta + q_g(dx\,dy\,dz)d\theta = (q_{x2} + q_{y2} + q_{z2})d\theta + \rho C_p\,dx\,dy\,dz\,dT \quad (6)$$

where dT is the change in temperature of the element during dθ, or $dT = dt/d\theta$. Thus the temperature distrib ution curve will be a function of the three dimensions and time, i.e., $T = F(X, Y, Z, \theta)$.

The heat q_x conducted into the element across the face X_1 during dθ is expressed in equation (1) as:

$$q_{x1} = -K\,dz\,dy\left.\frac{\partial T}{\partial x}\right|_{x1} \quad (7)$$

It is necessary to express the temperature gradient as a partial derivative since T is a function not only of X but also of Y and Z. It is easily shown that the rate of heat flow across the face X_2 can be expressed as:

$$q_{x2} = \left[-K\left.\frac{\partial T}{\partial x}\right|_{x1} + \frac{\partial}{\partial x}\left(-K\frac{\partial t}{\partial x}\right)dx\right]dz\,dy \quad (8)$$

Subtracting equation 8 from 7 gives:

$$q_{x1} - q_{x2} = \left[\frac{\partial}{\partial x}\left(K\frac{\partial T}{\partial x}\right)\right]dx\,dy\,dz \quad (9)$$

Similar expressions can be written for the Y and Z direction accordingly.

$$q_{z1} - q_{z2} = \left[\frac{\partial}{\partial z}\left(K\frac{\partial T}{\partial z}\right)\right] dx\,dz\,dy \tag{10}$$

$$q_{y1} - q_{y2} = \left[\frac{\partial}{\partial y}\left(K\frac{\partial T}{\partial y}\right)\right] dx\,dz\,dy \tag{11}$$

Substituting equation 9, 10 and 11 into the energy balance equation and disregarding any internal heat source and dividing each term by dxdzdy yields:

$$\frac{\partial}{\partial x}\left(K\frac{\partial T}{\partial x}\right) + \frac{\partial}{\partial z}\left(K\frac{\partial T}{\partial z}\right) + \frac{\partial}{\partial y}\left(K\frac{\partial T}{\partial y}\right) = c_p \rho \frac{\partial T}{\partial \theta} \tag{12}$$

If the temperature difference between points 1 and 2, i.e., X_1, X_2, Z_1, Z_2, and Y_1, Y_2 is not too great then Cp, and k can be considered constant over the temperature range T_1 to T_2. Making the assumption of constancy and dividing equation (2) by k gives:

$$\frac{\partial^2 T}{\partial x^2} + \frac{\partial^2 T}{\partial z^2} + \frac{\partial^2 T}{\partial y^2} = \frac{c_p \rho}{K} \frac{\partial T}{\partial \theta} \tag{13}$$

Setting $k/c_p\rho = H$, (thermal diffusivity) and substituting into equation (13) gives the Fourier heat transfer equation

$$\frac{\partial^2 T}{\partial X^2} + \frac{\partial^2 T}{\partial Z^2} + \frac{\partial^2 T}{\partial Y^2} = \frac{1}{H}\frac{\partial T}{\partial \theta}. \tag{14}$$

If the rod is carried to a steady state, i.e., $\frac{\partial T}{\partial \theta} = 0$ then the result is the Laplace heat transfer equation

$$\frac{\partial^2 T}{\partial X^2} + \frac{\partial^2 T}{\partial Z^2} + \frac{\partial^2 T}{\partial Y^2} = 0. \tag{15}$$

Since the heat flow in the rods used for this research was in one direction, equation (14) reduces to

$$\frac{\partial^2 T}{\partial X^2} = \frac{1}{H}\frac{\partial T}{\partial \theta}. \tag{16}$$

Unsteady state temperature profiles are available on the specimen used in this research; however, H was calculated as:

$$H = \frac{K}{C_p \rho}. \tag{17}$$

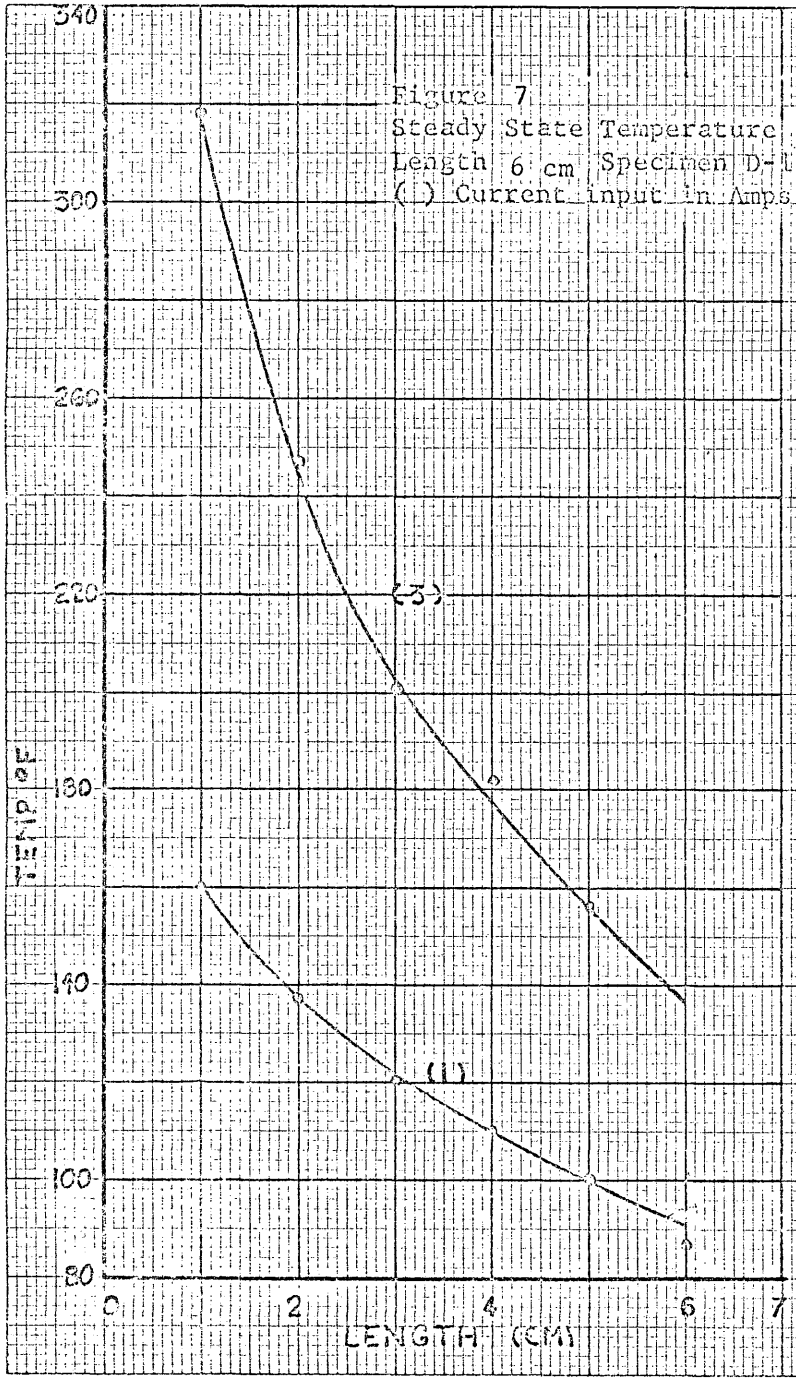

Figure 7
Steady State Temperature
Length 6 cm Specimen D-1
( ) Current Input in Amps

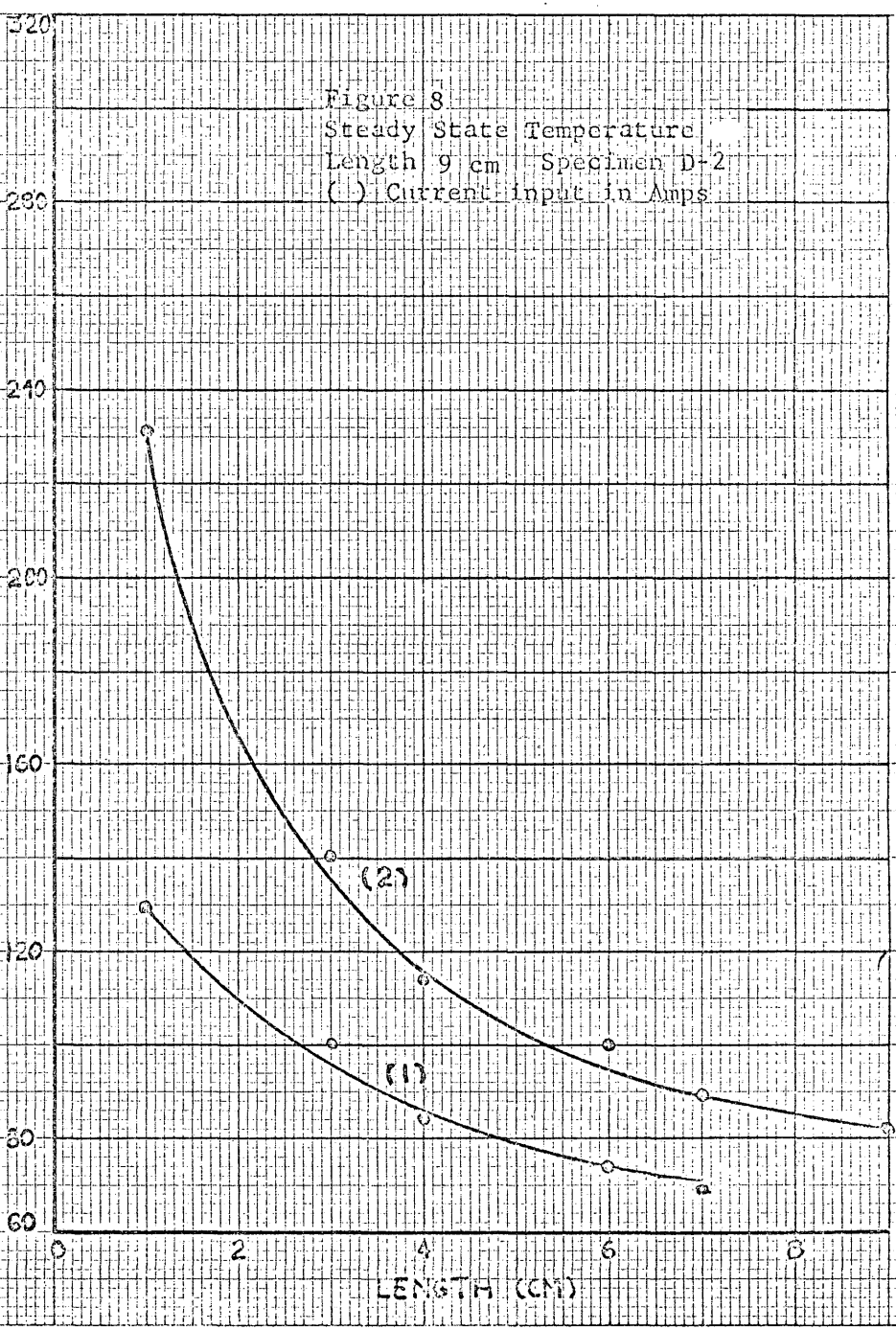

Figure 8
Steady State Temperature
Length 9 cm Specimen D-2
( ) Current Input in Amps

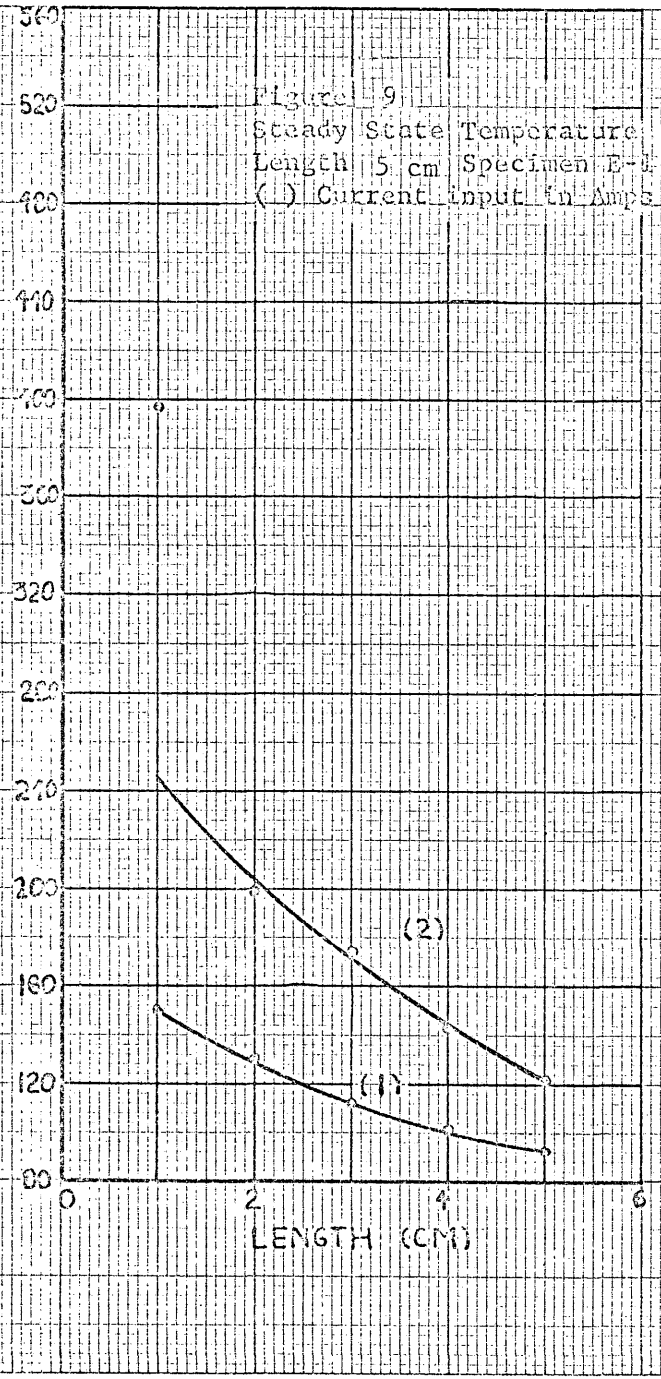

Figure 9
Steady State Temperature
Length 5 cm Specimen E-1
( ) Current Input in Amps

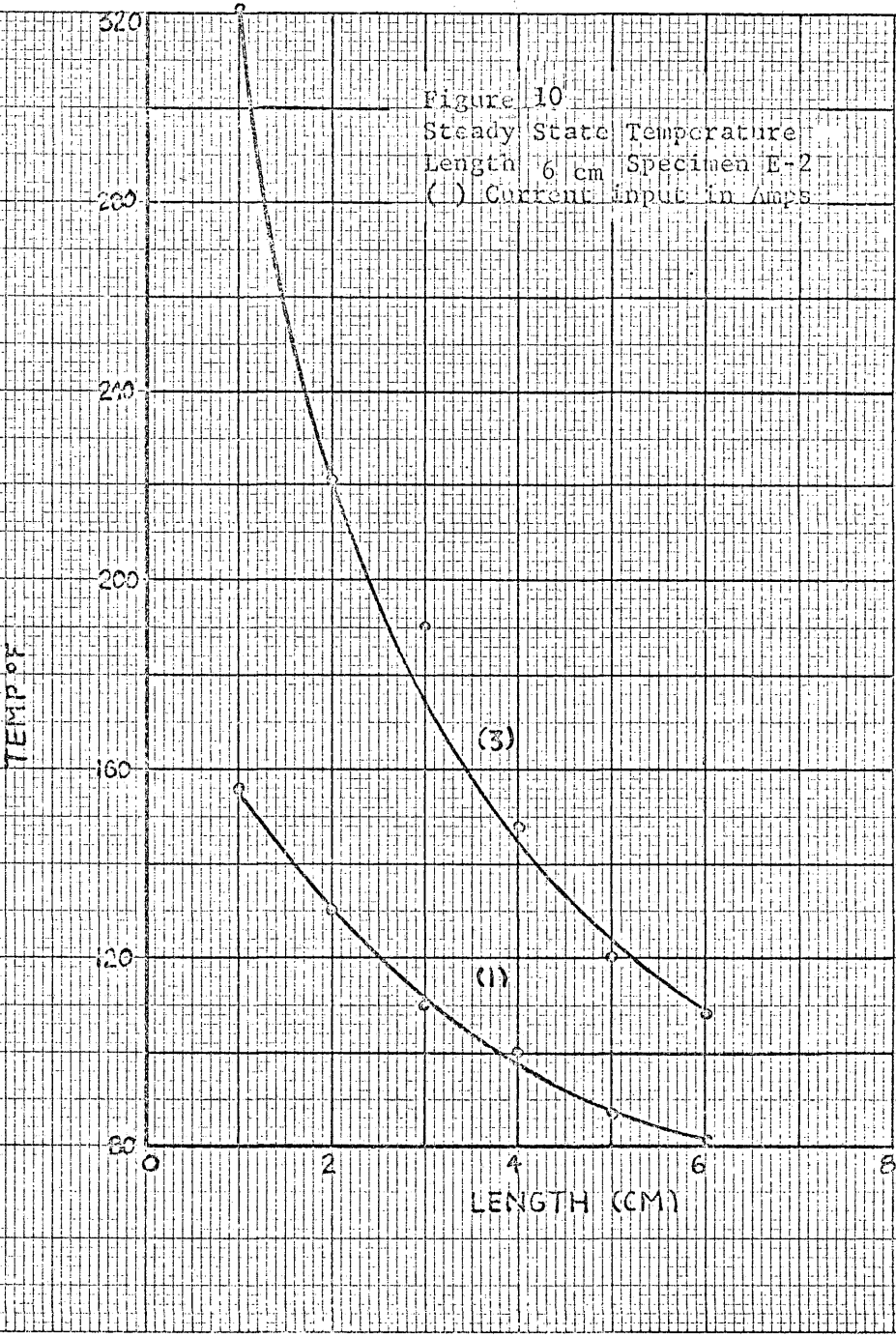

Figure 10
Steady State Temperature
Length 6 cm Specimen E-2
( ) Current Input in Amps

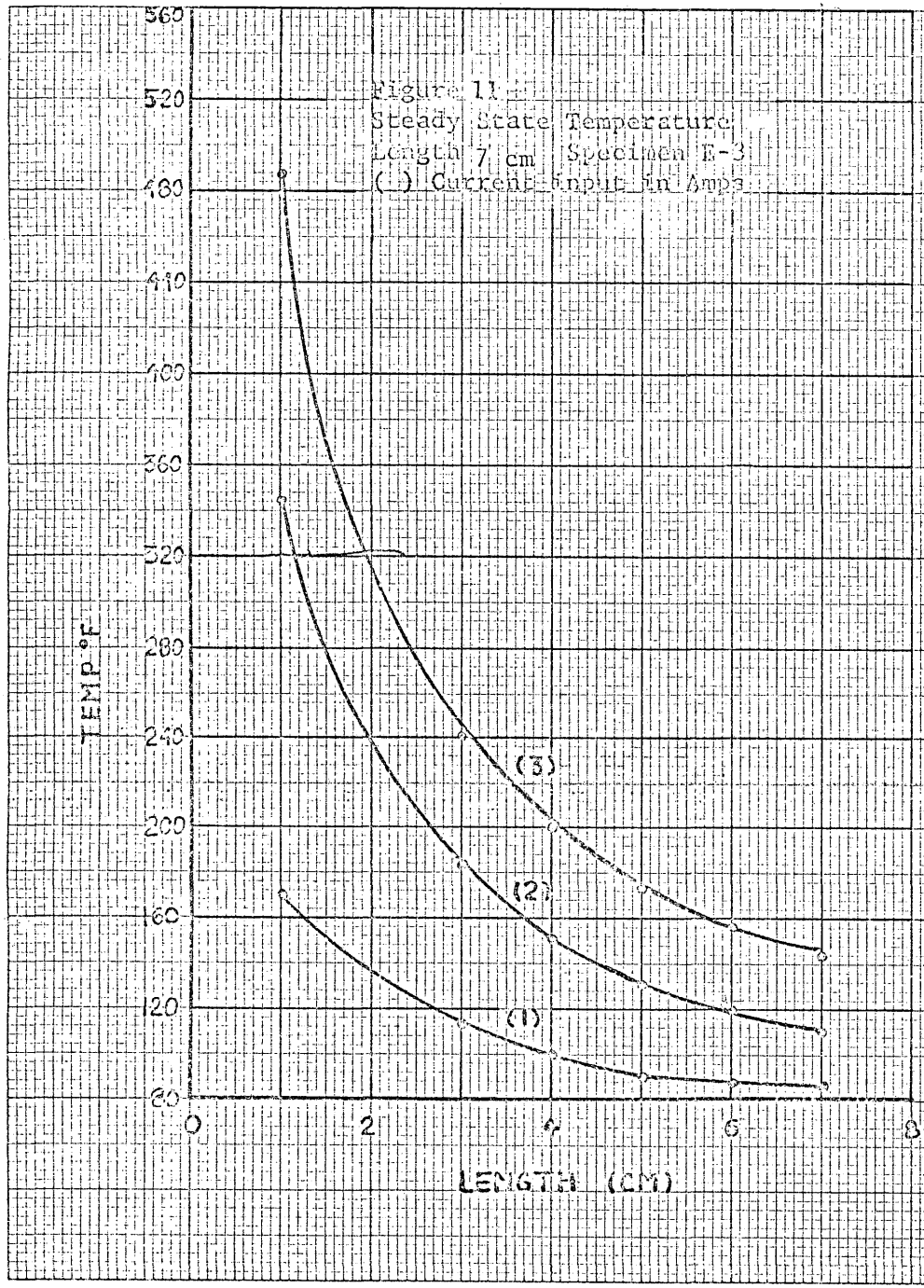

Figure 11
Steady State Temperature
Length 7 cm Specimen E-3
( ) Current Input in Amps

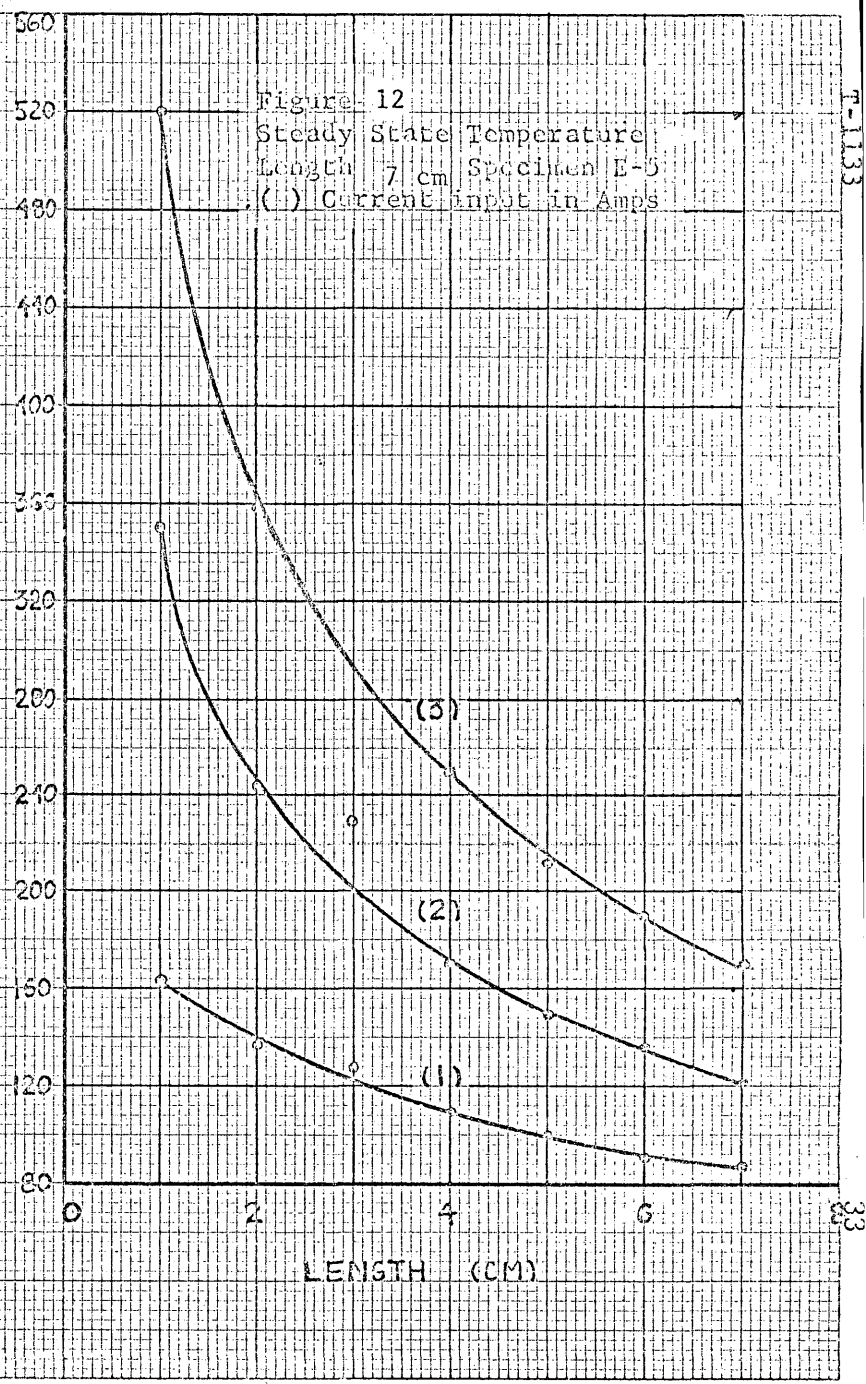

Figure 12
Steady State Temperature
Length 7 cm Specimen E-5
( ) Current Input in Amps

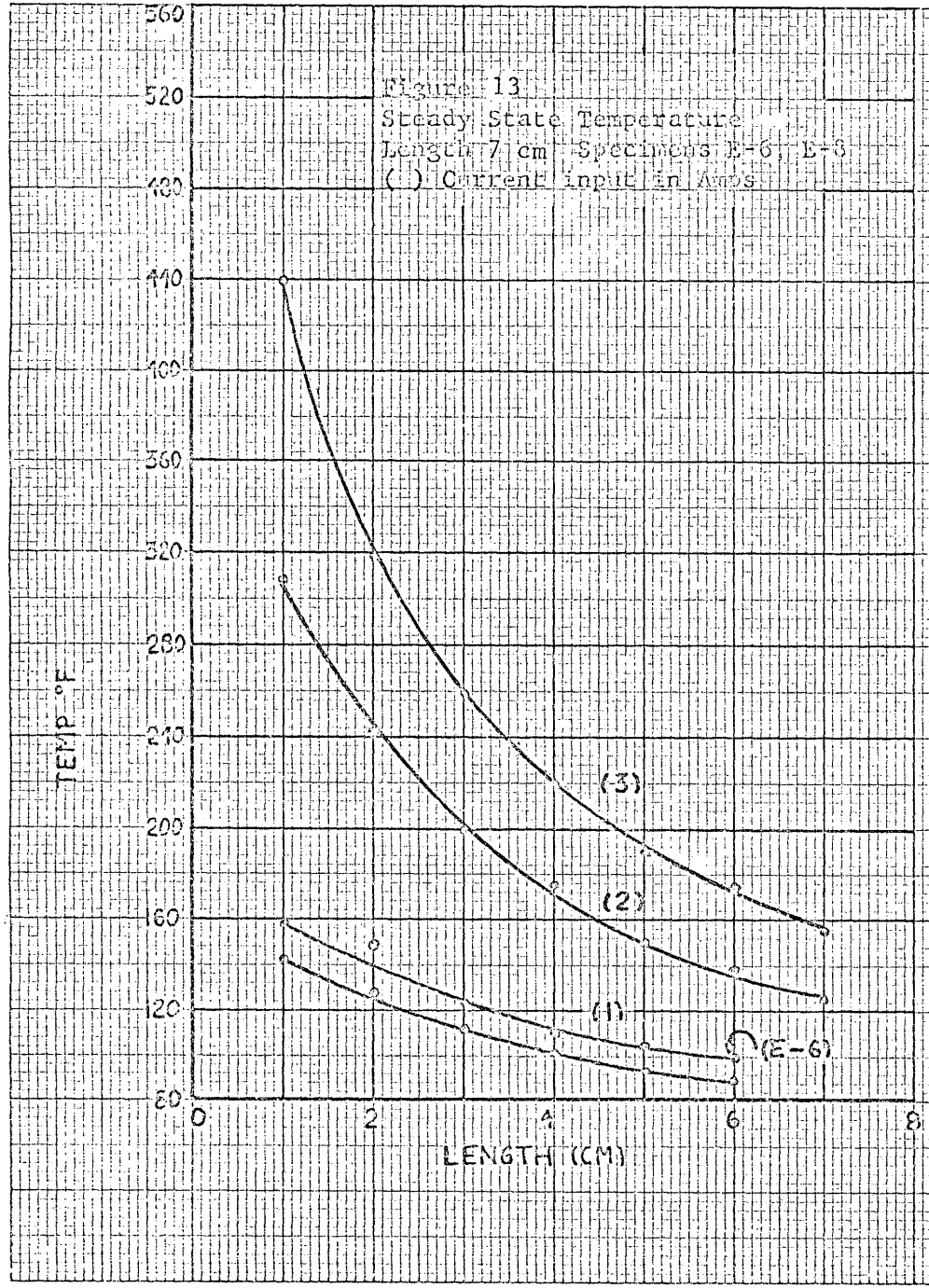

Figure 13
Steady State Temperature
Length 7 cm Specimens E-6, E-8
( ) Current input in Amps

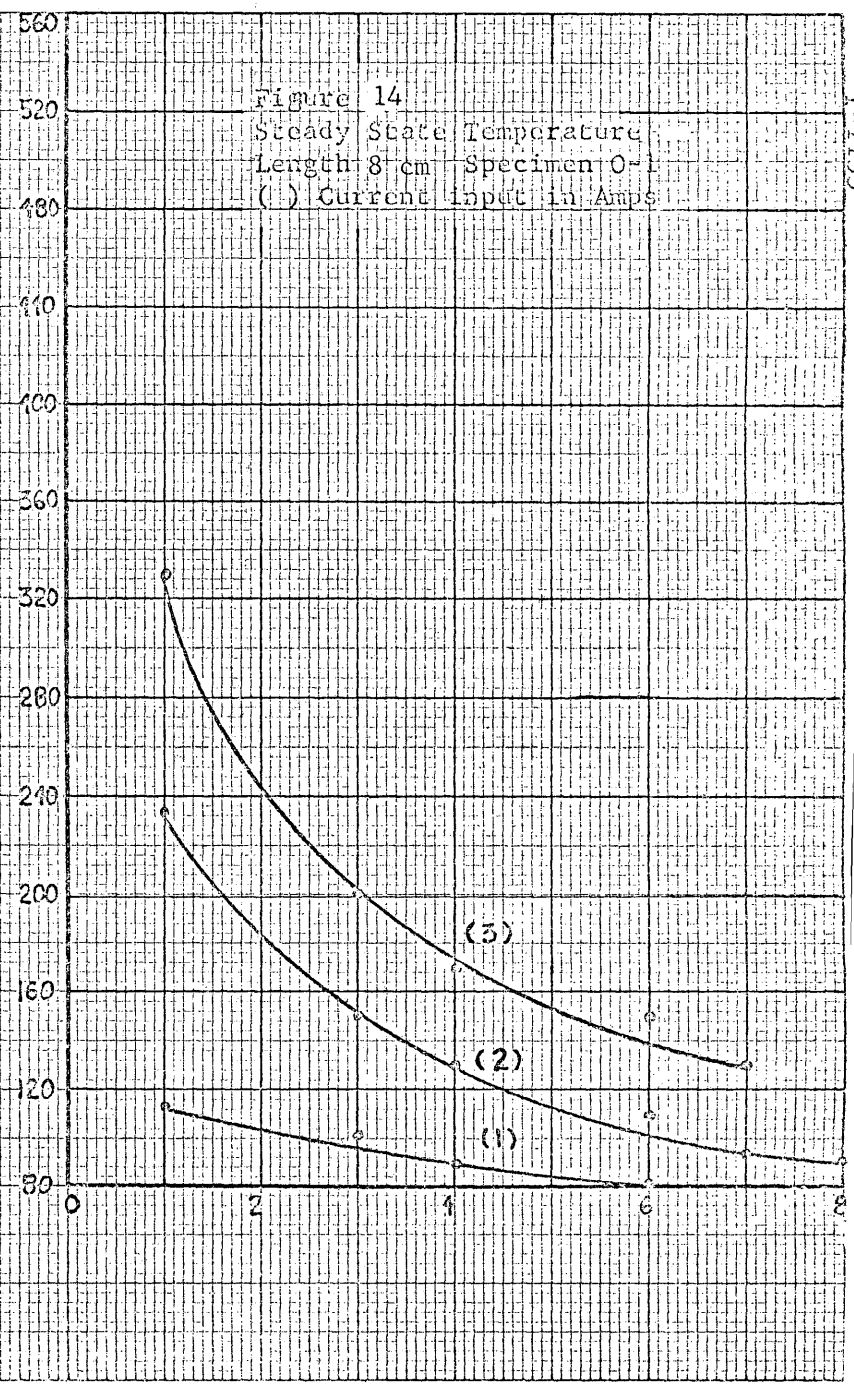

Figure 14
Steady State Temperature
Length 8 cm Specimen O-1
( ) Current input in Amps

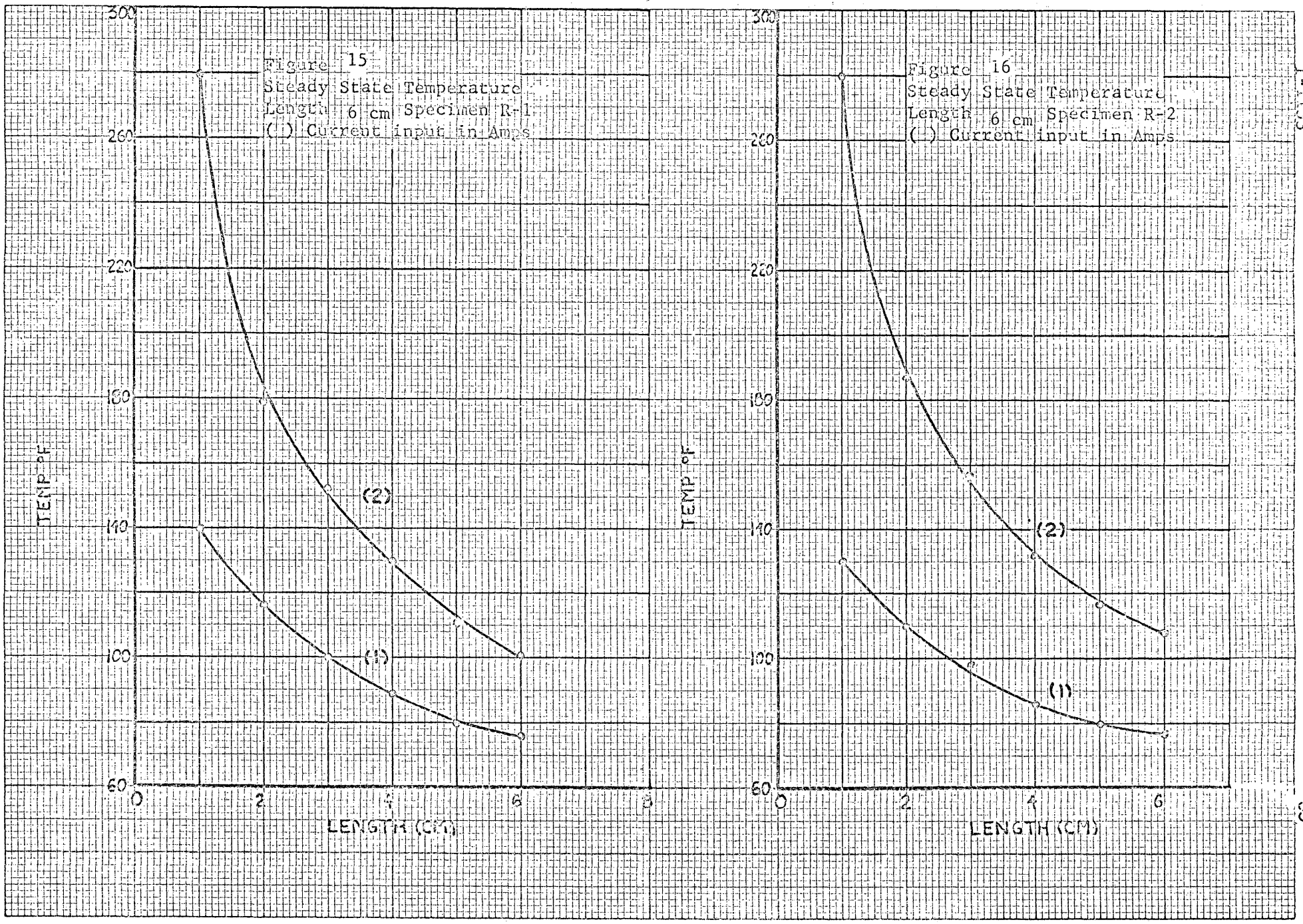

Figure 15
Steady State Temperature
Length 6 cm Specimen R-1
( ) Current input in Amps

Figure 16
Steady State Temperature
Length 6 cm Specimen R-2
( ) Current input in Amps

Figure 17
Steady State Temperature
Length 6 cm Specimen S-1
( ) Current input in Amps

Figure 18
Steady State Temperature
Length 6 cm Specimen S-1A
( ) Current input in Amps

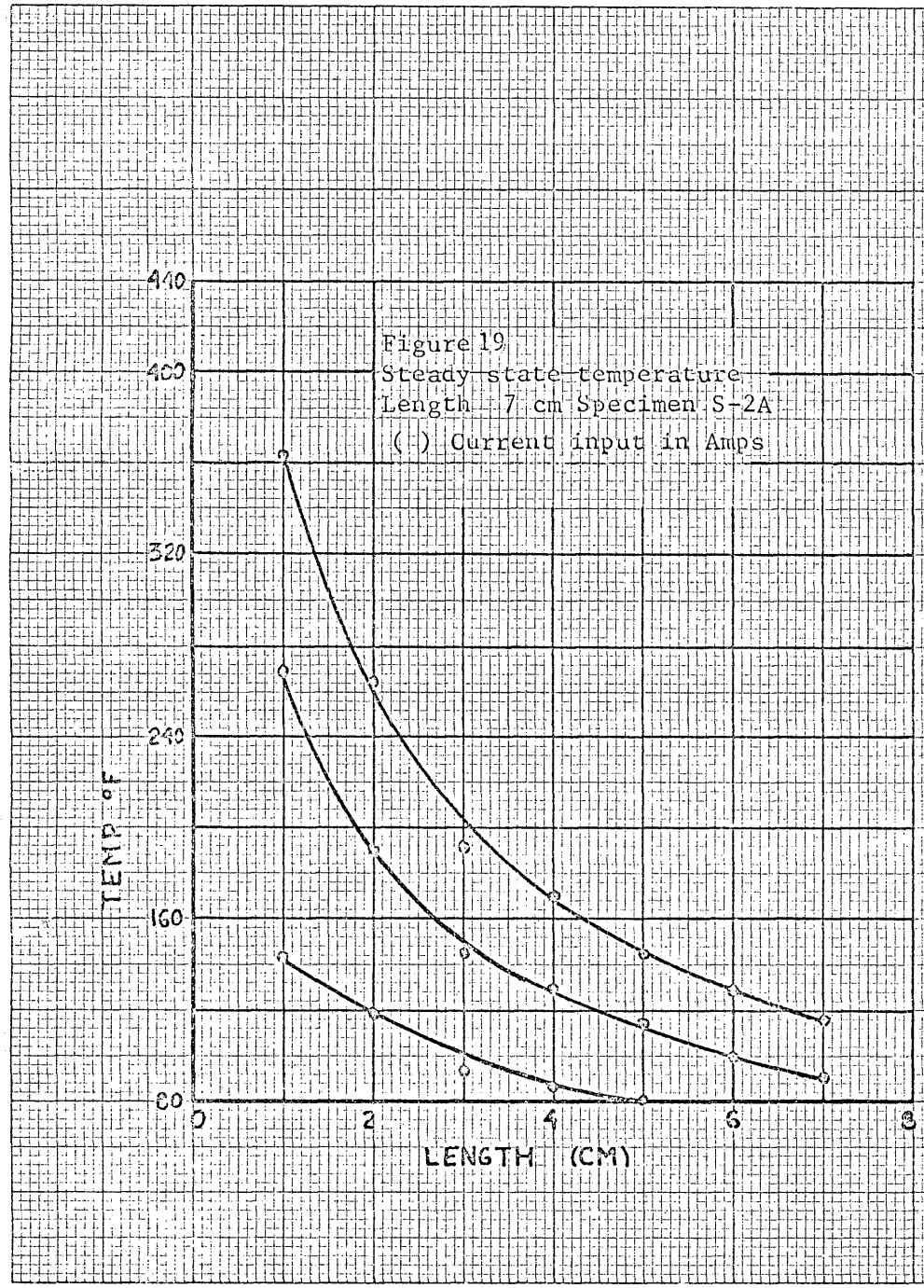

Figure 19
Steady state temperature
Length 7 cm Specimen S-2A
( ) Current input in Amps

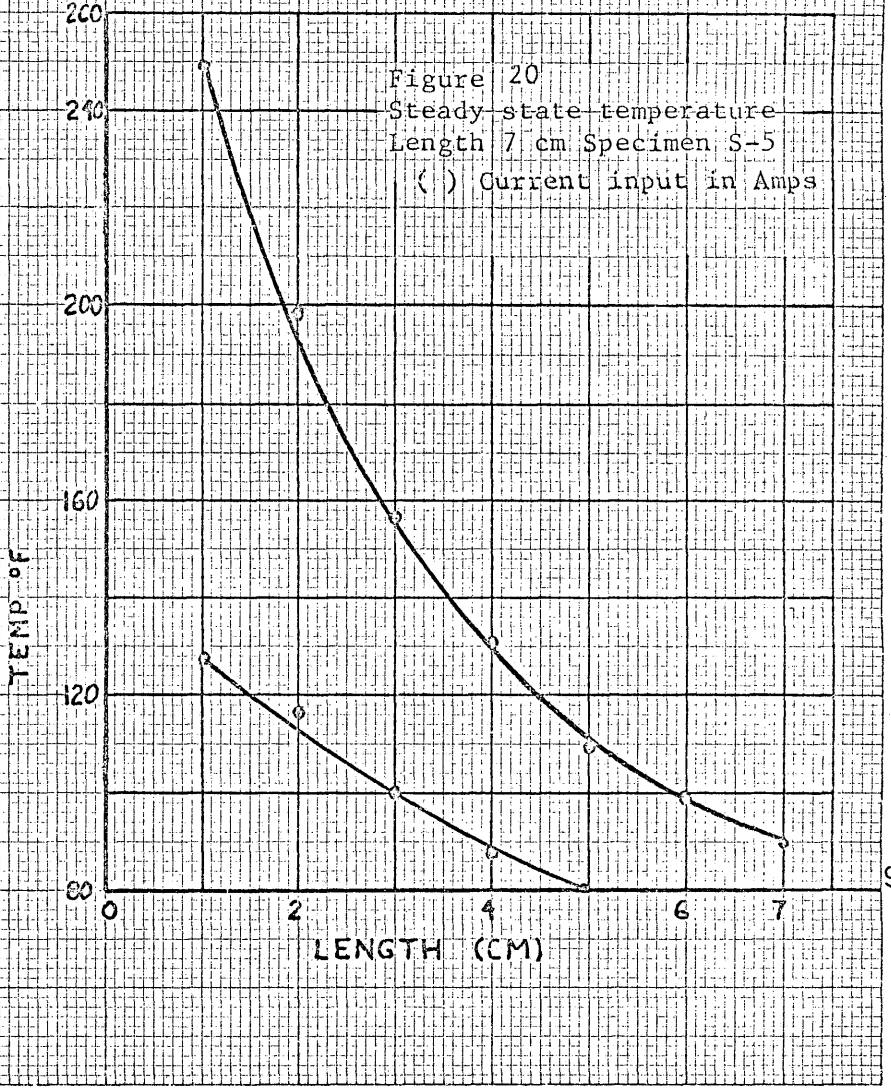

Figure 20
Steady state temperature
Length 7 cm Specimen S-5
( ) Current input in Amps

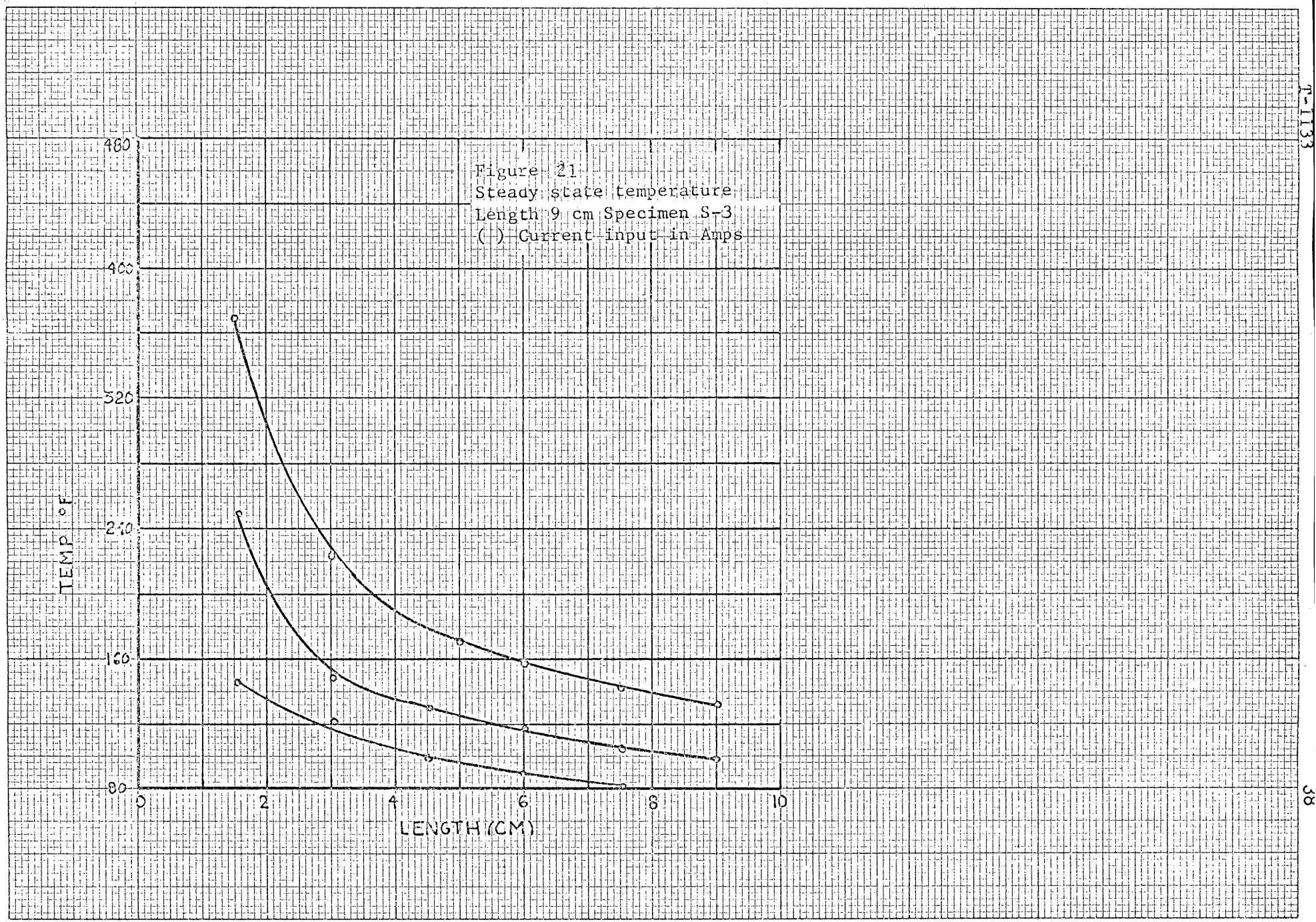

Figure 21
Steady state temperature
Length 9 cm Specimen S-3
( ) Current input in Amps

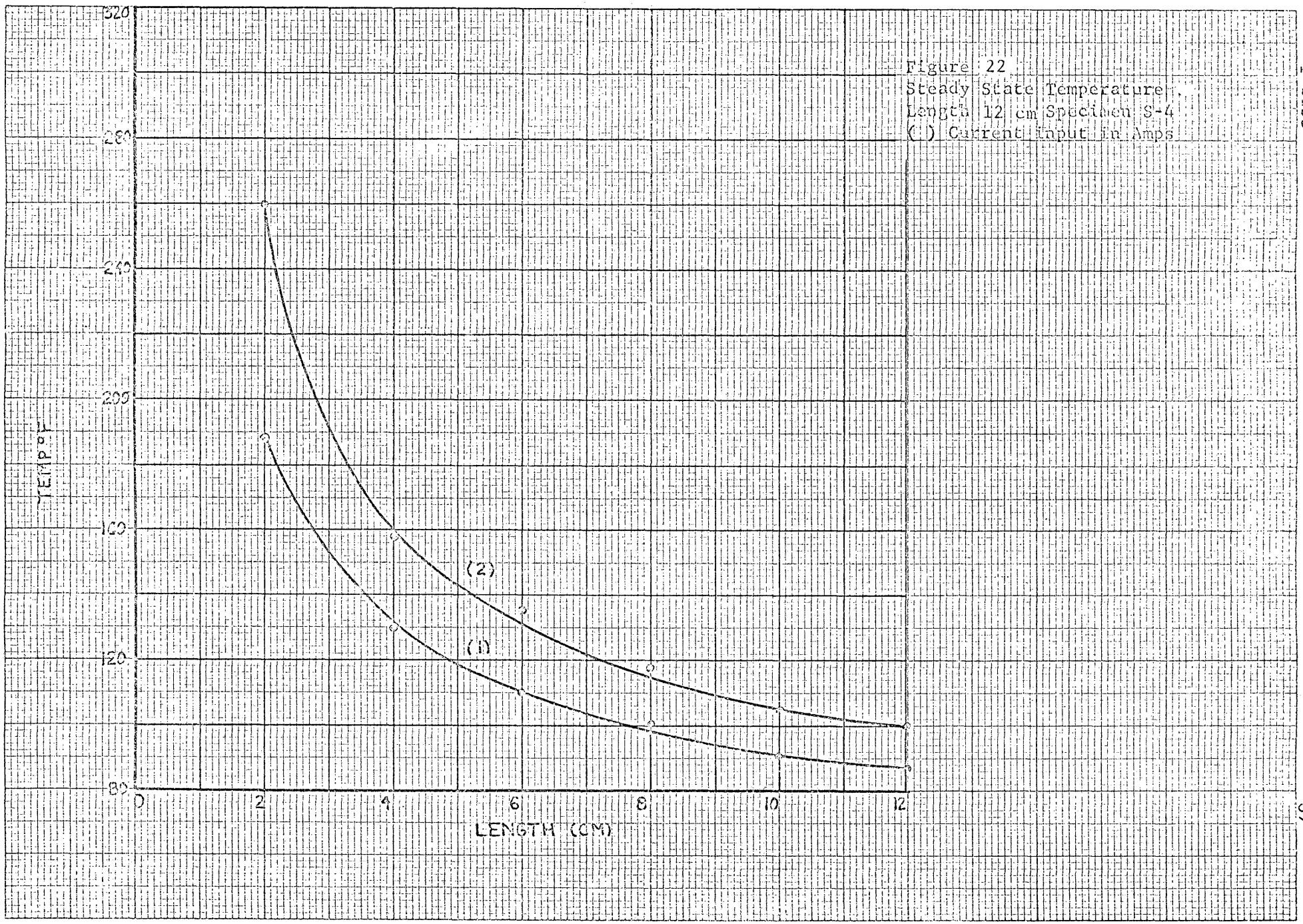

Figure 22
Steady State Temperature
Length 12 cm Specimen S-4
( ) Current Input in Amps

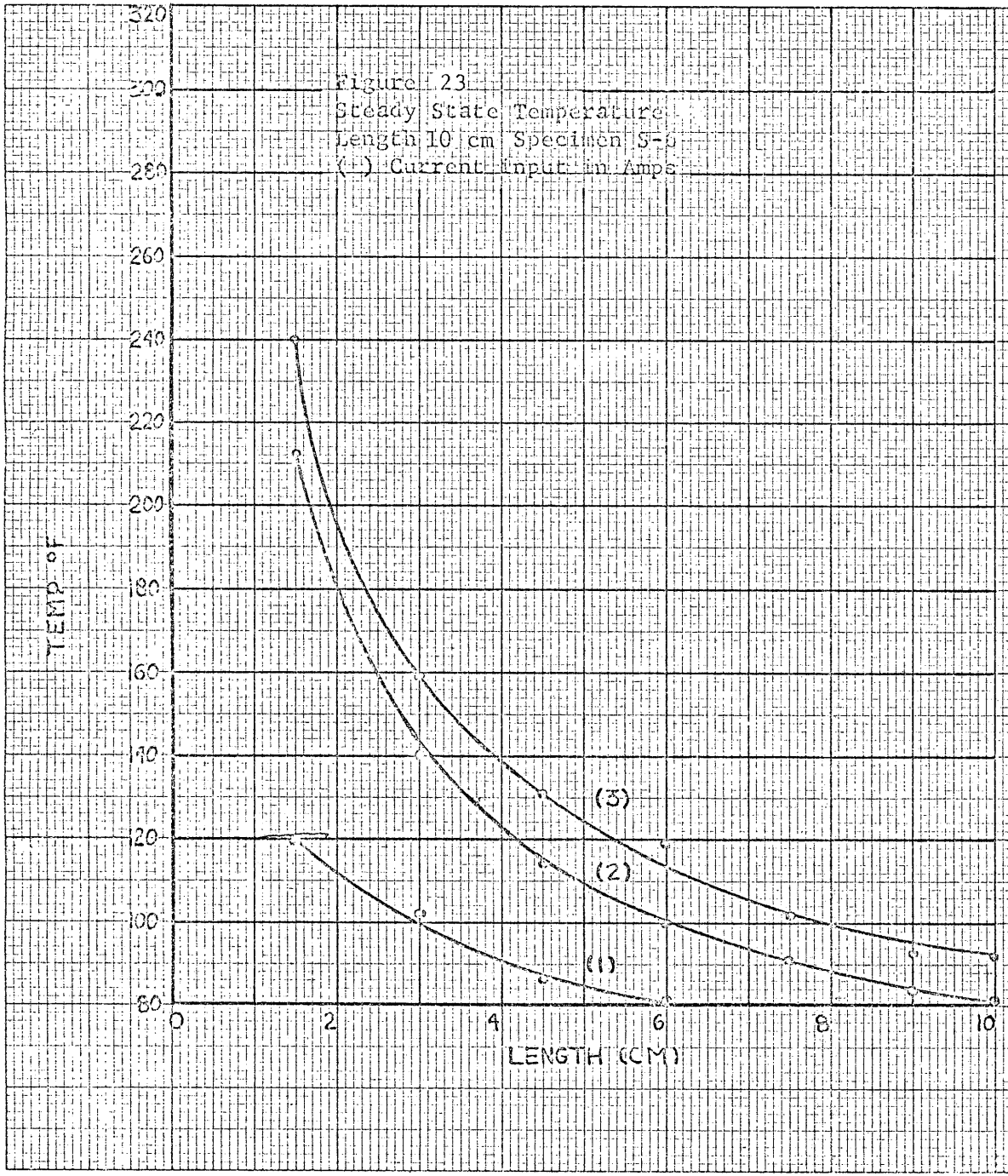

Figure 23
Steady State Temperature
Length 10 cm Specimen S-6
( ) Current Input in Amps

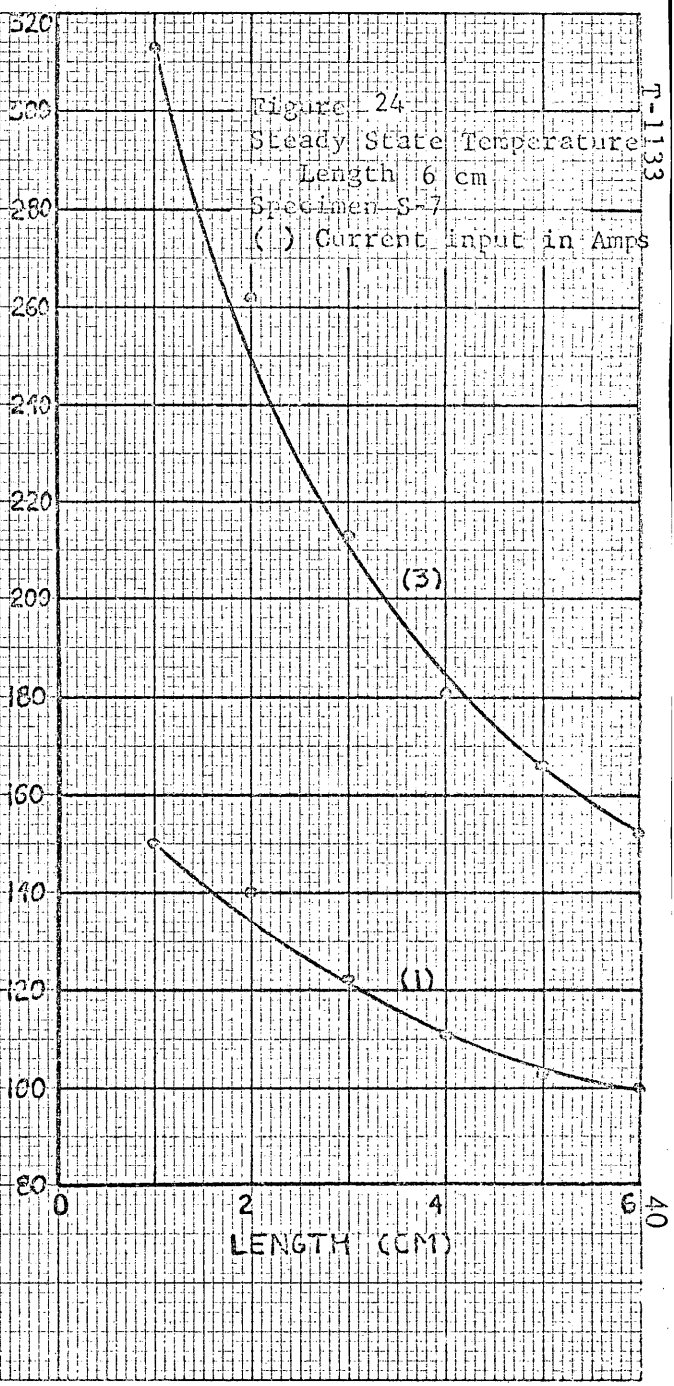

Figure 24
Steady State Temperature
Length 6 cm
Specimen S-7
( ) Current Input in Amps

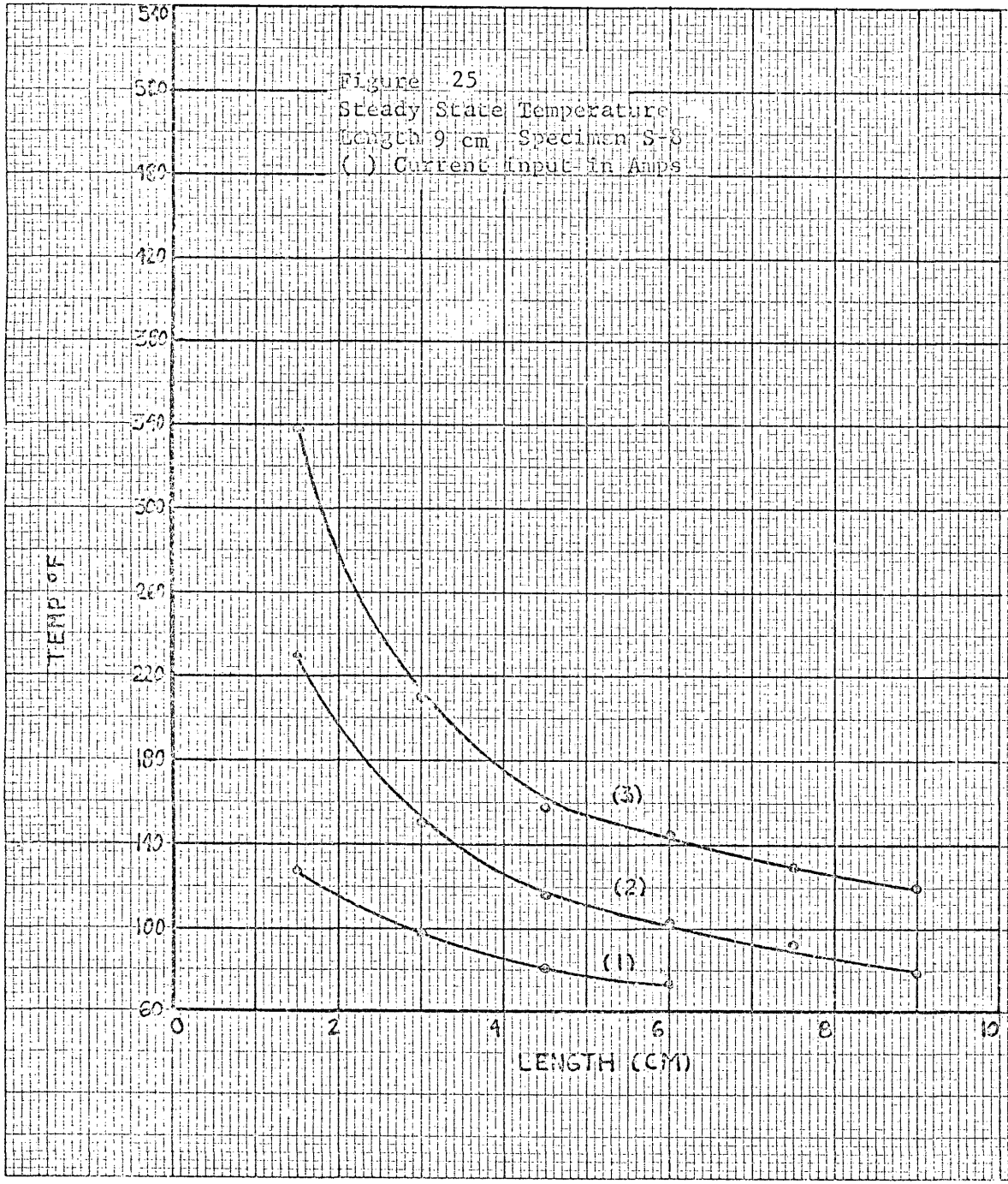

Figure 25
Steady State Temperature
Length 9 cm Specimen S-8
( ) Current Input in Amps

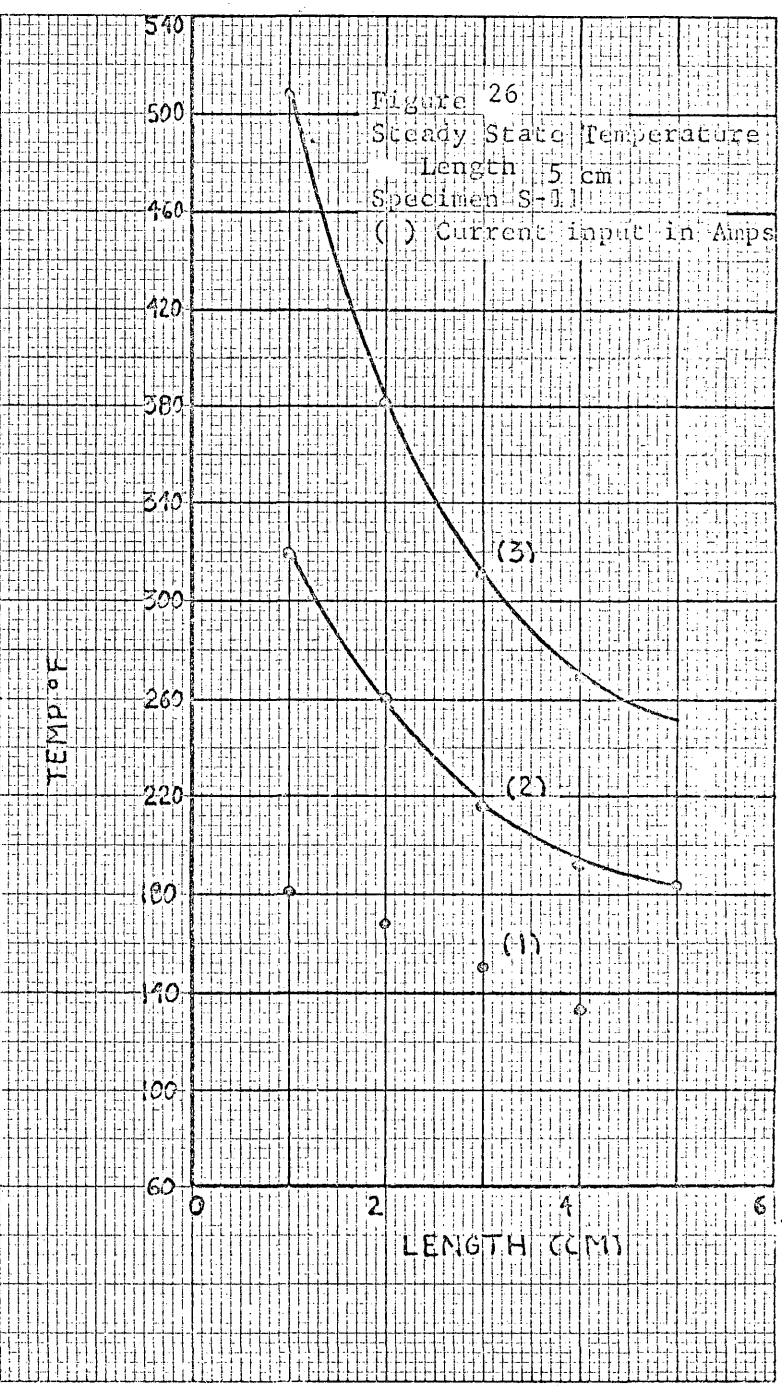

Figure 26
Steady State Temperature
Length 5 cm
Specimen S-11
( ) Current Input in Amps

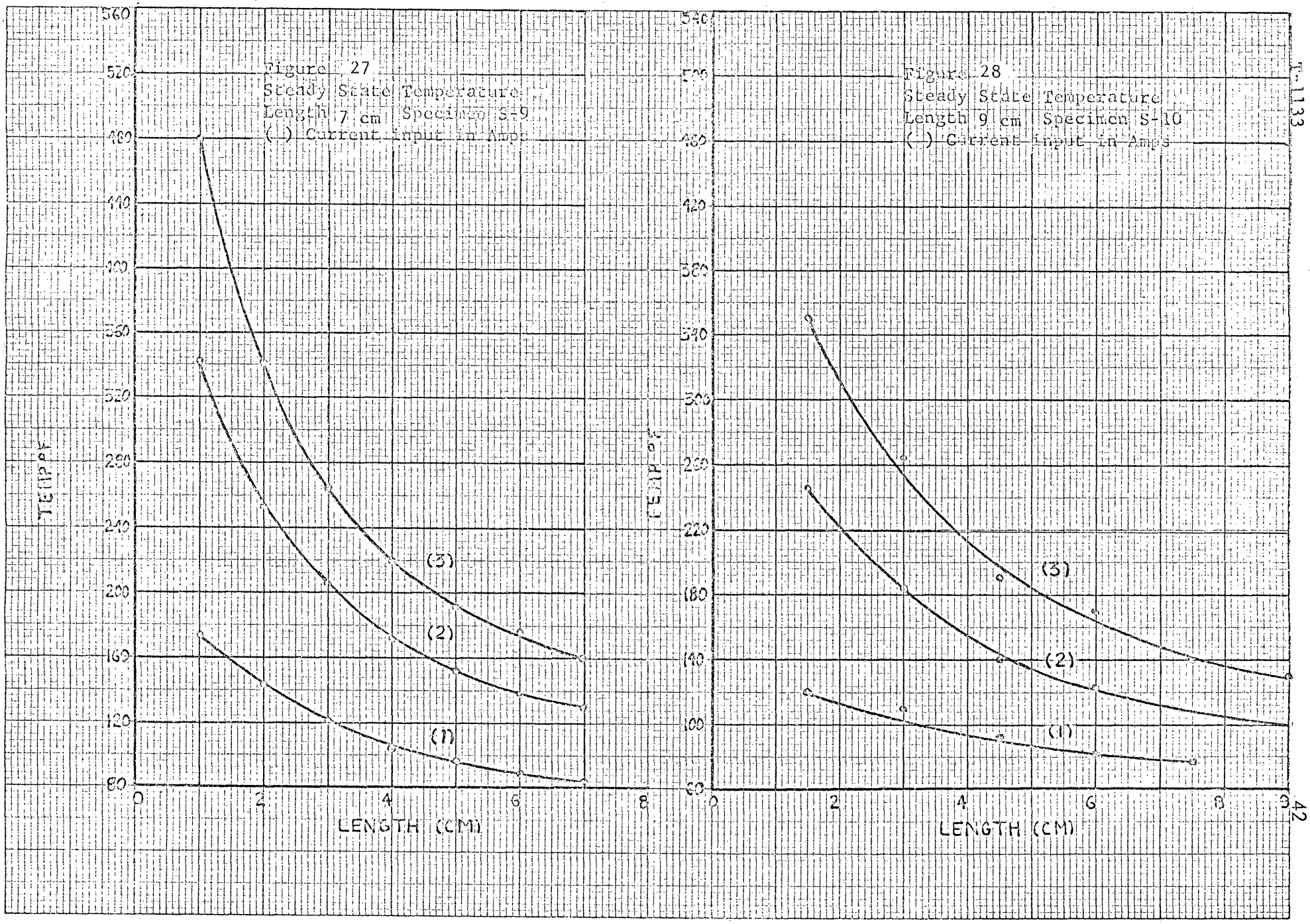

Figure 27
Steady State Temperature
Length 7 cm Specimen S-9
( ) Current Input in Amps

Figure 28
Steady State Temperature
Length 9 cm Specimen S-10
( ) Current Input in Amps

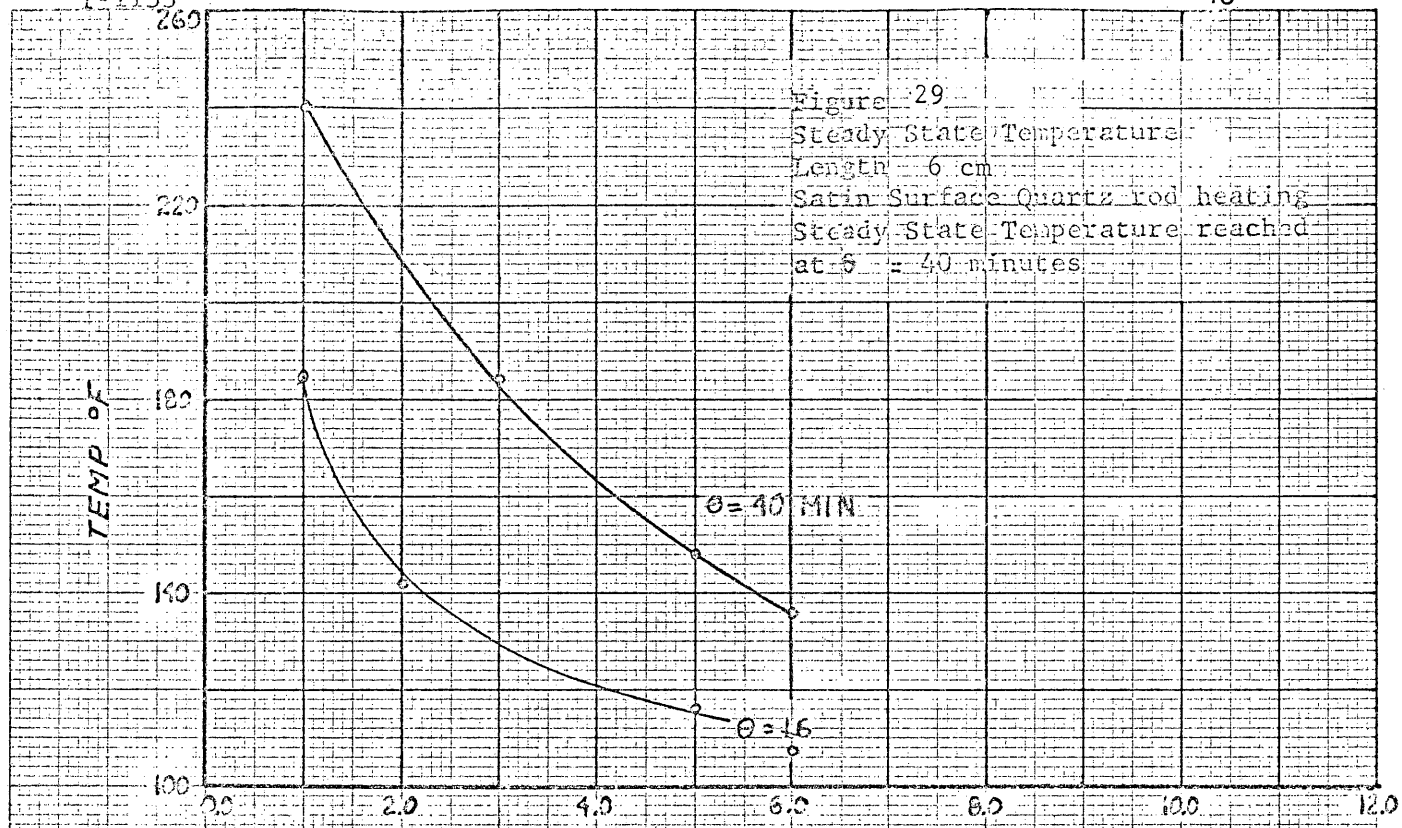

Figure 29
Steady State Temperature
Length 6 cm
Satin Surface Quartz rod heating
Steady State Temperature reached
at θ = 40 minutes

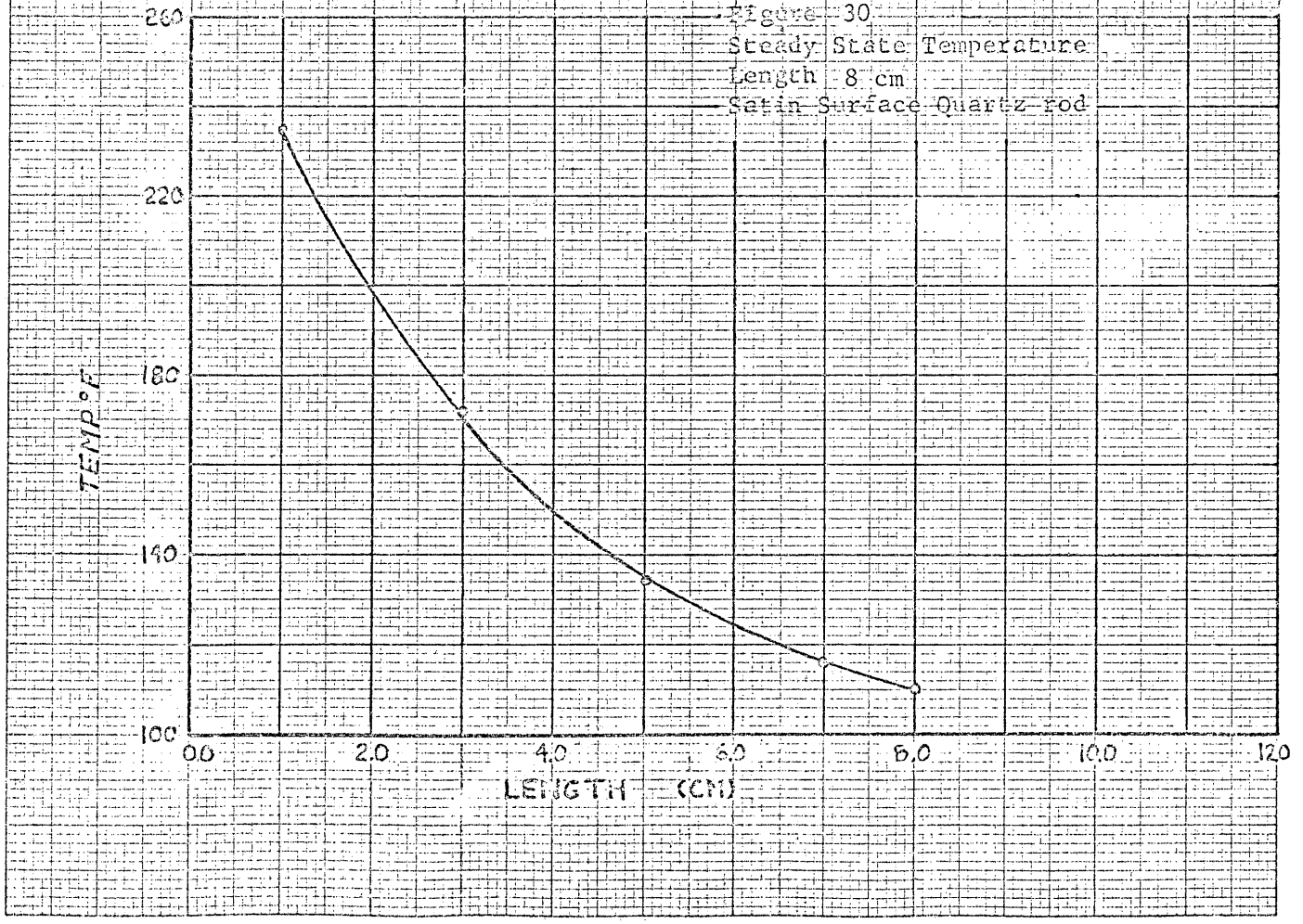

Figure 30
Steady State Temperature
Length 8 cm
Satin Surface Quartz rod

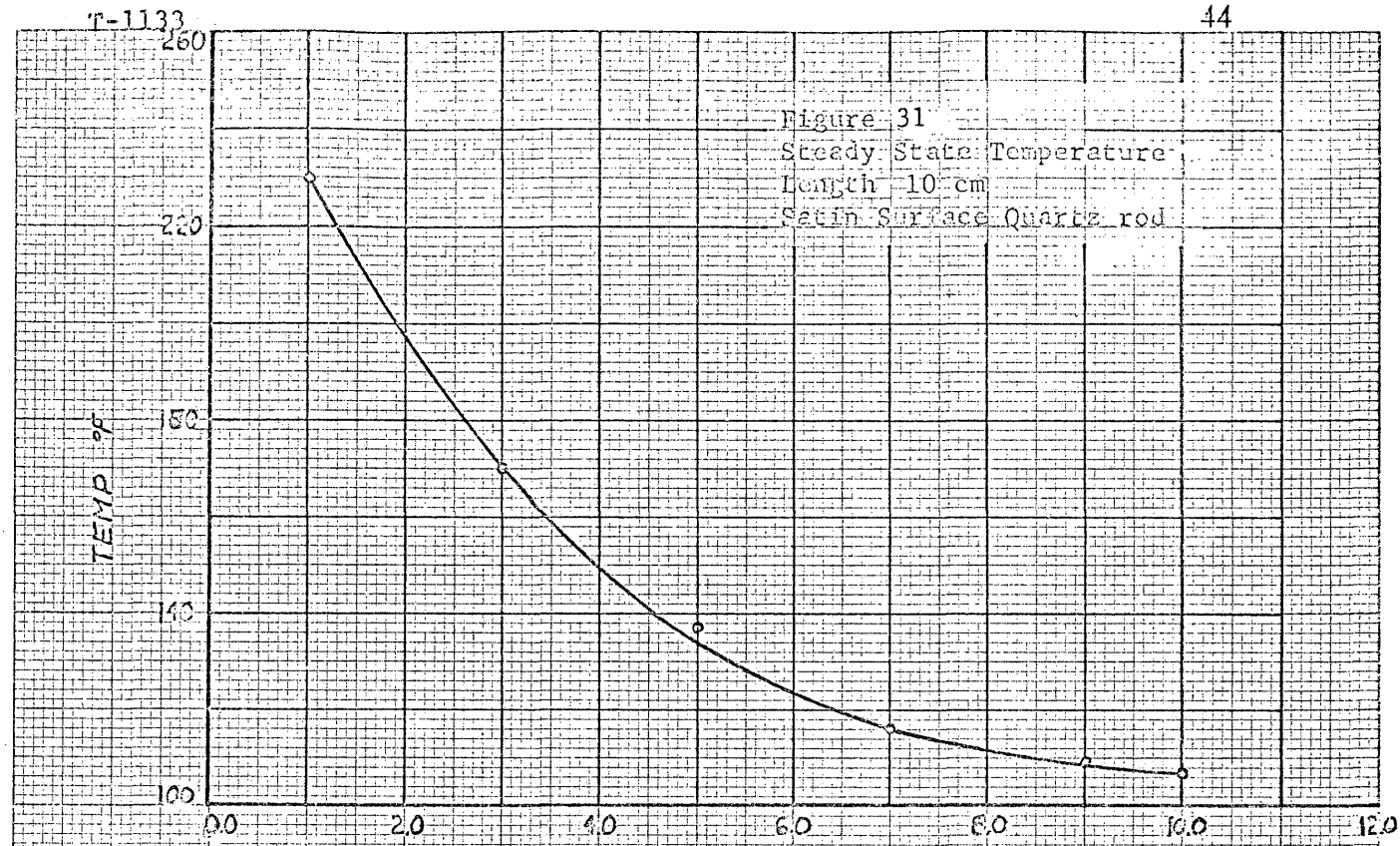

Figure 31
Steady State Temperature
Length 10 cm
Satin Surface Quartz rod

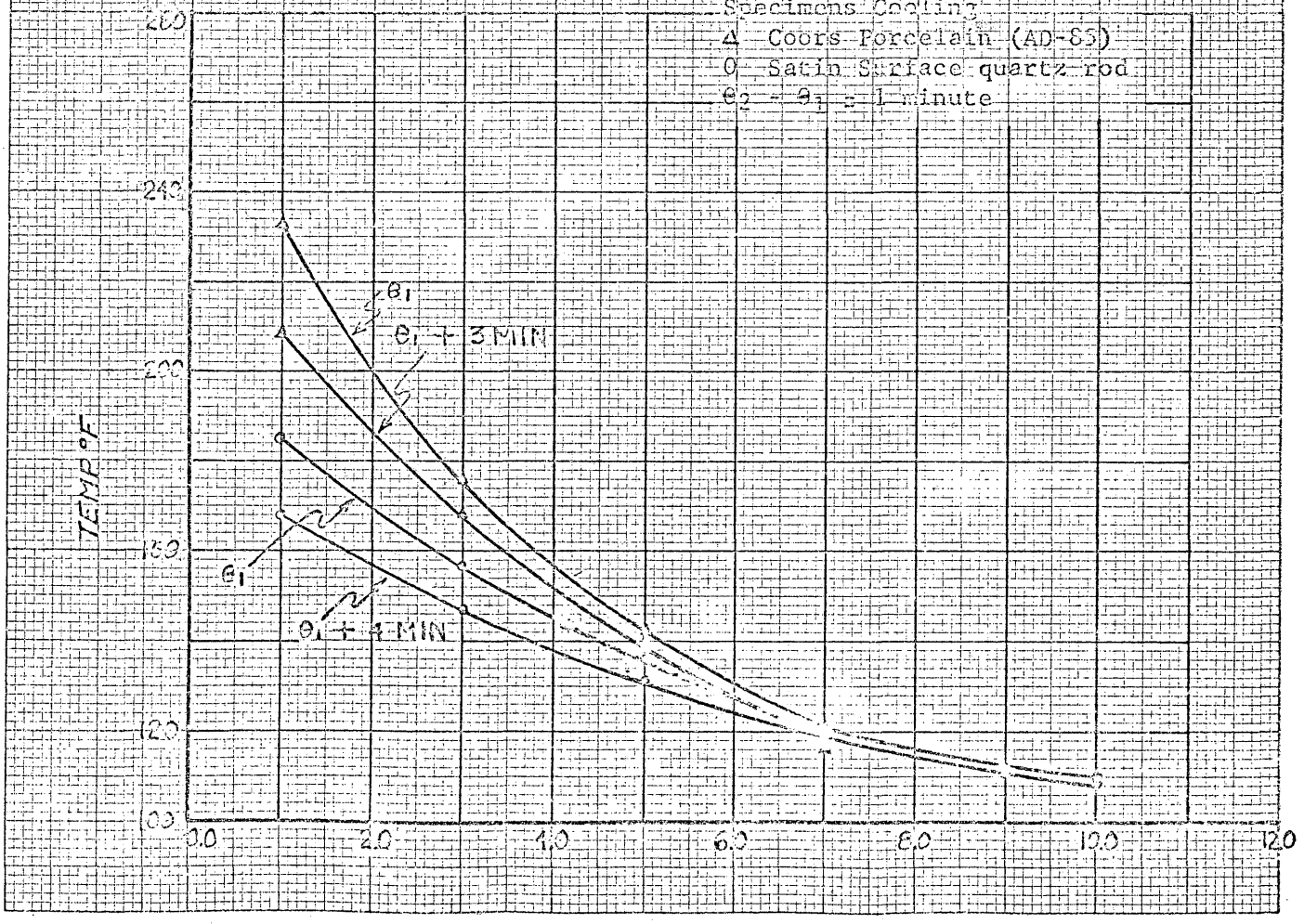

Figure 32
Temperature - Length 10 cm
Specimens Cooling
Δ Coors Porcelain (AD-85)
○ Satin Surface quartz rod
$\theta_2 - \theta_1 = 1$ minute

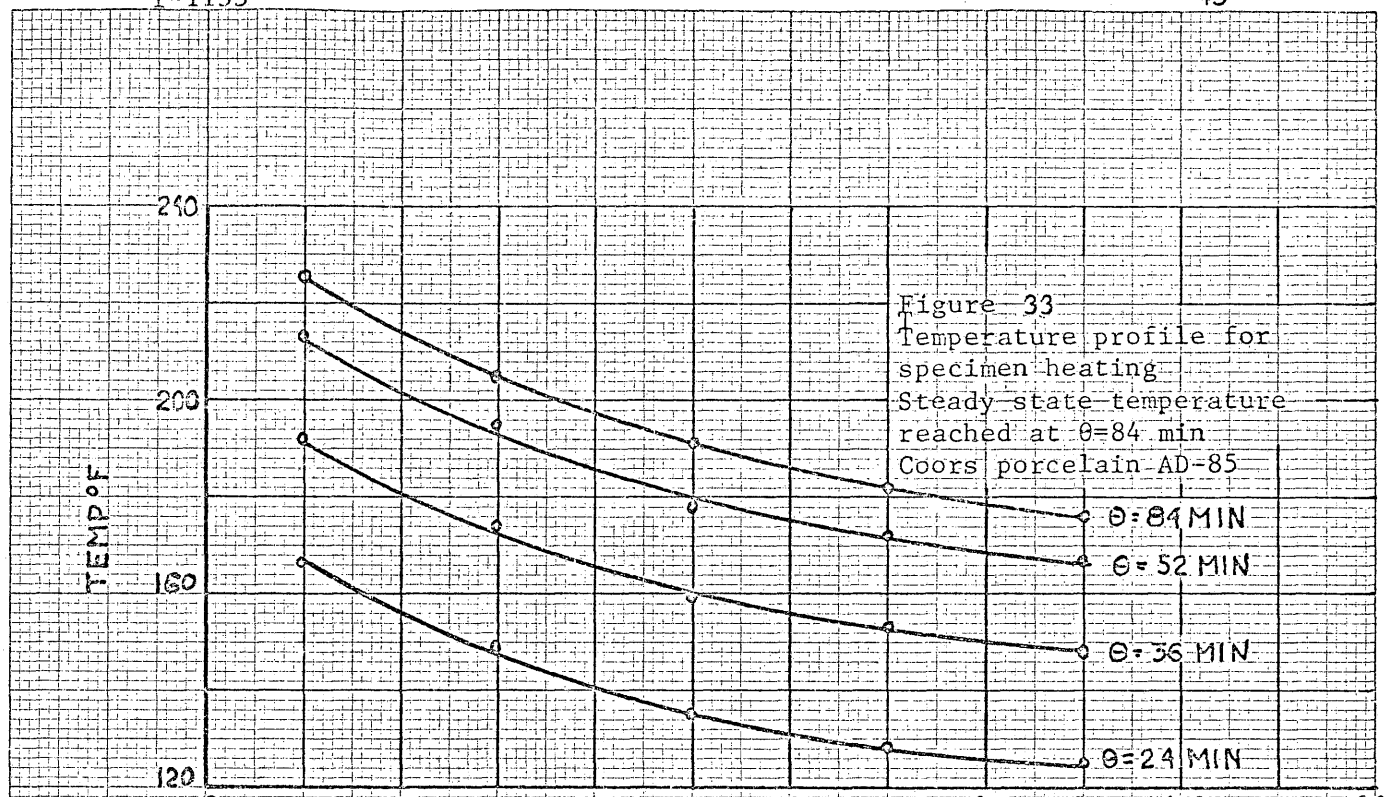

Figure 33
Temperature profile for specimen heating
Steady state temperature reached at θ=84 min
Coors porcelain AD-85

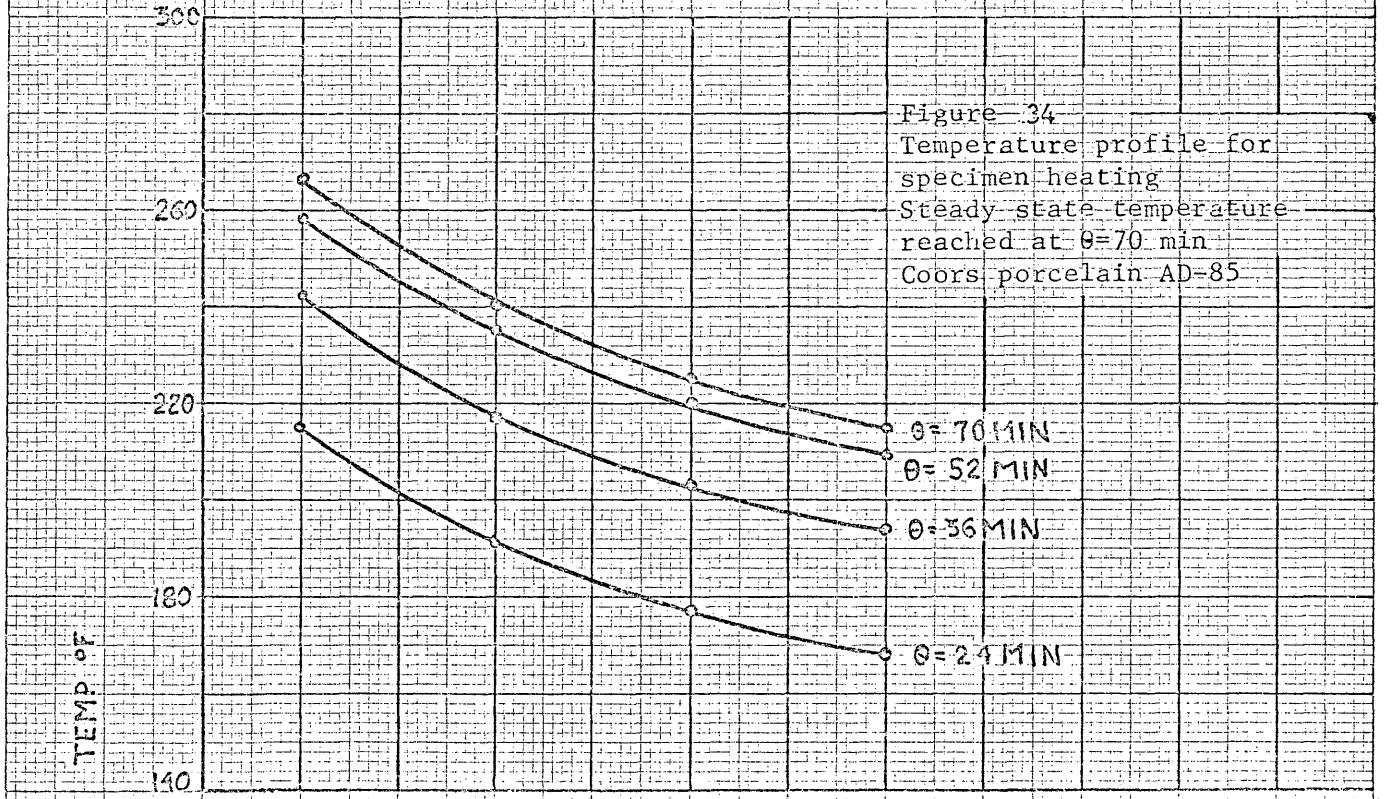

Figure 34
Temperature profile for specimen heating
Steady state temperature reached at θ=70 min
Coors porcelain AD-85

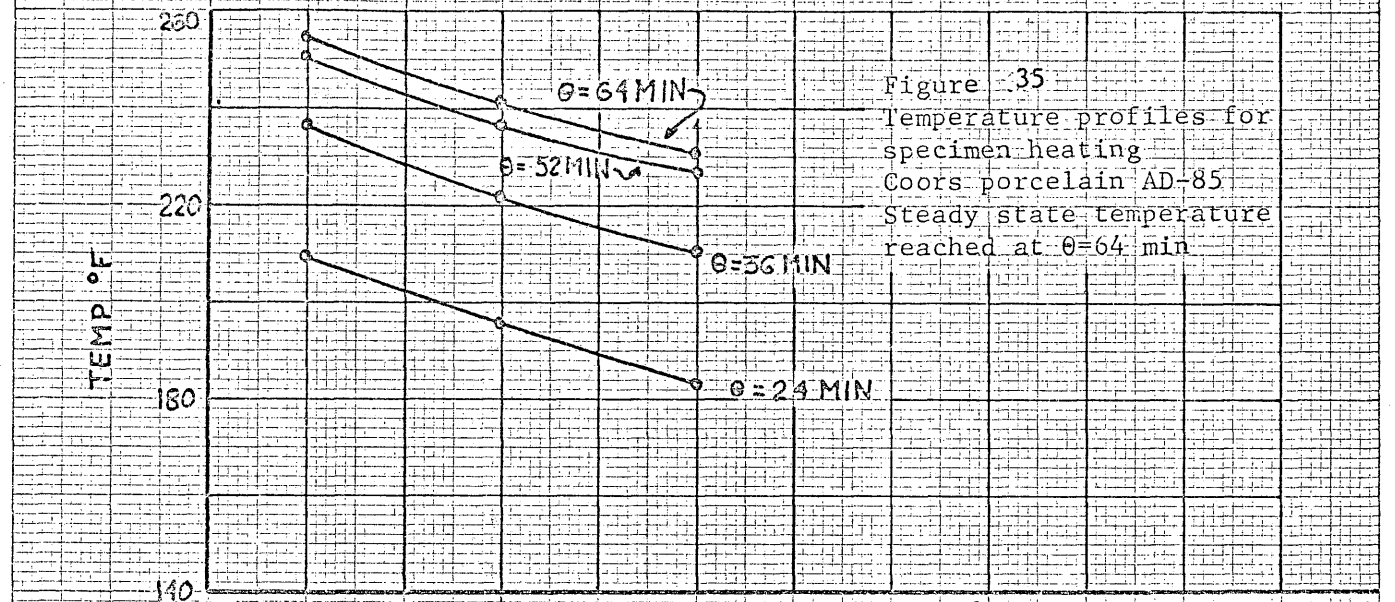

Figure 35
Temperature profiles for specimen heating
Coors porcelain AD-85
Steady state temperature reached at θ=64 min

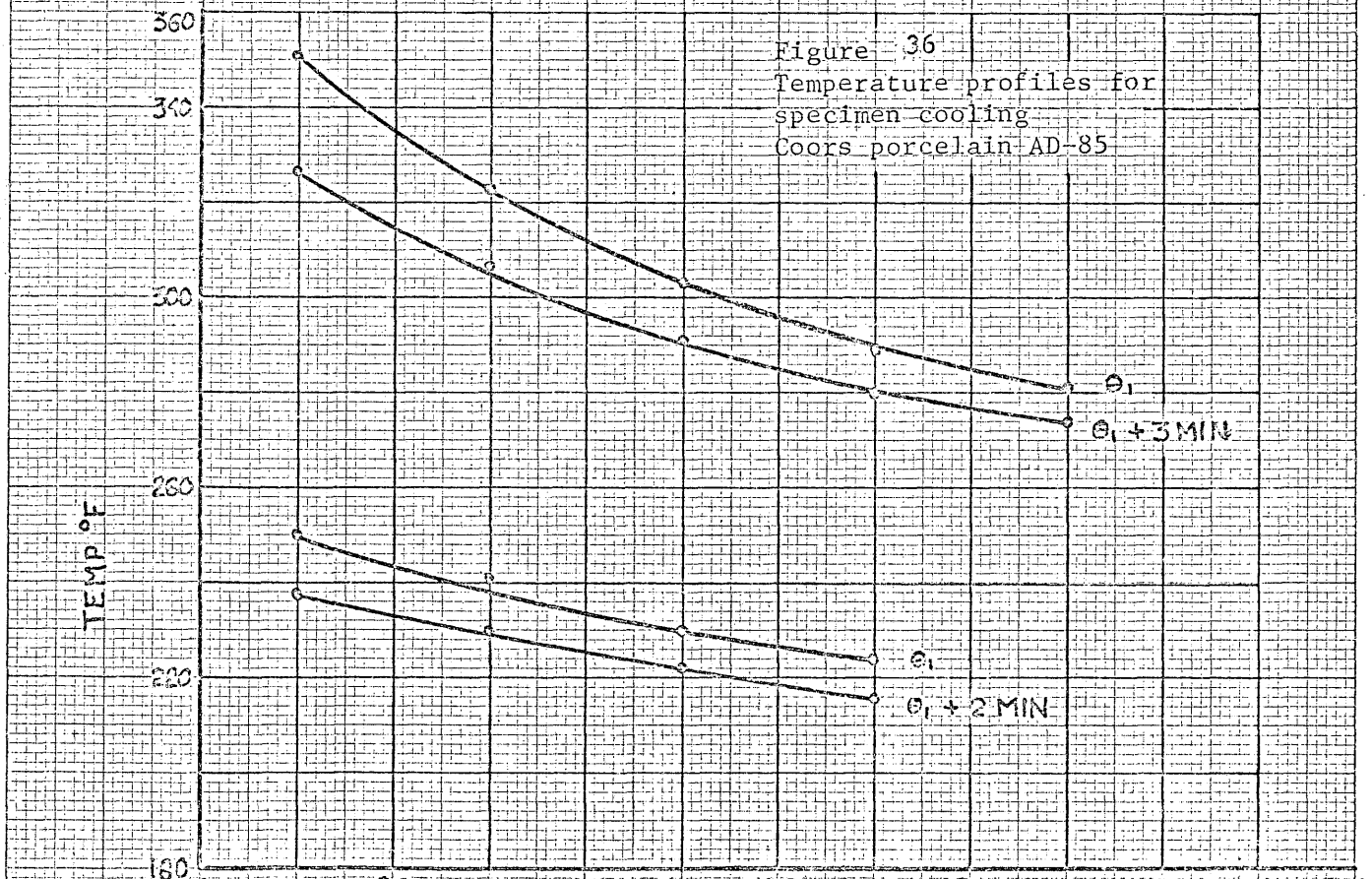

Figure 36
Temperature profiles for specimen cooling
Coors porcelain AD-85

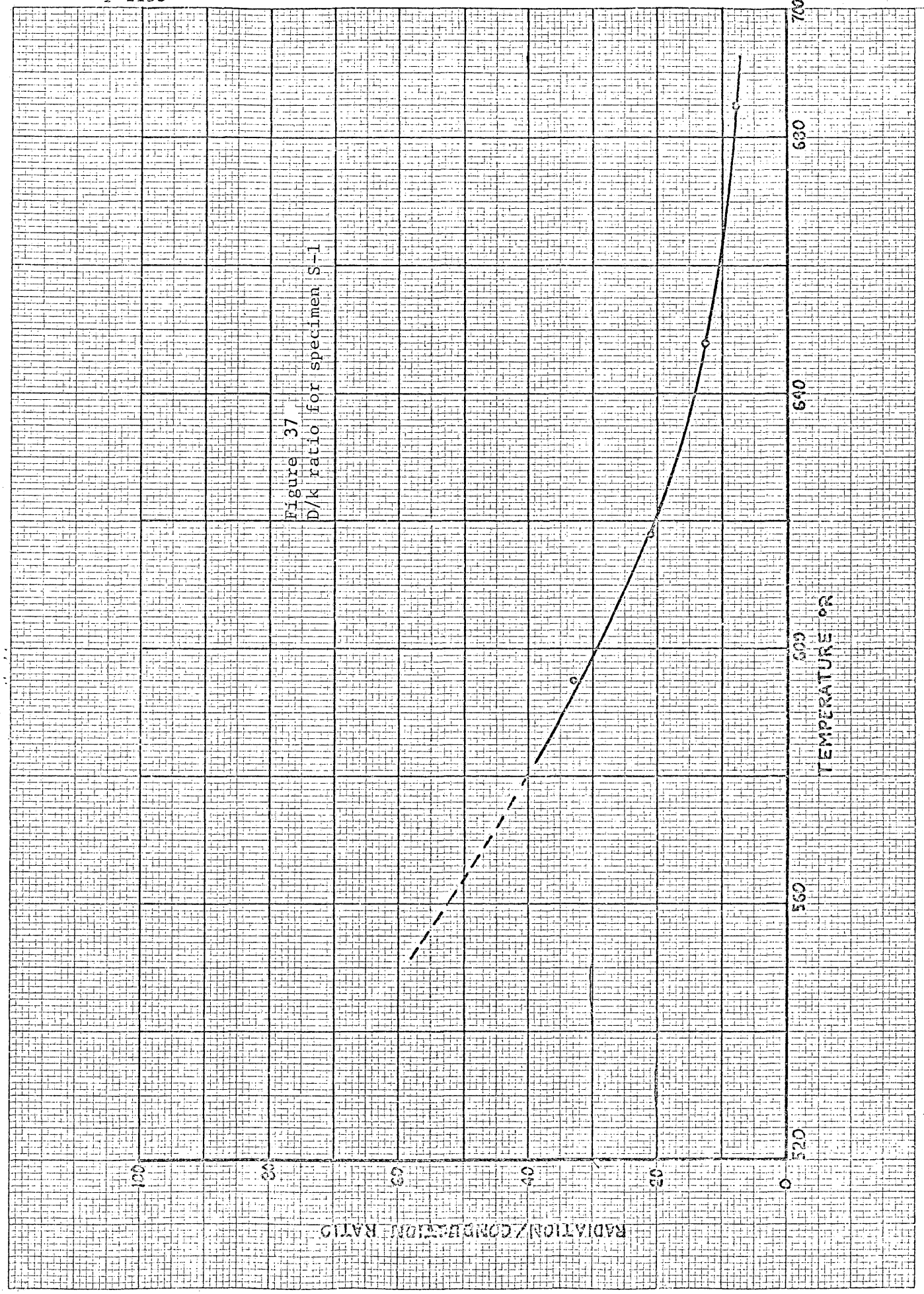

Figure 37
D/k ratio for specimen S-1

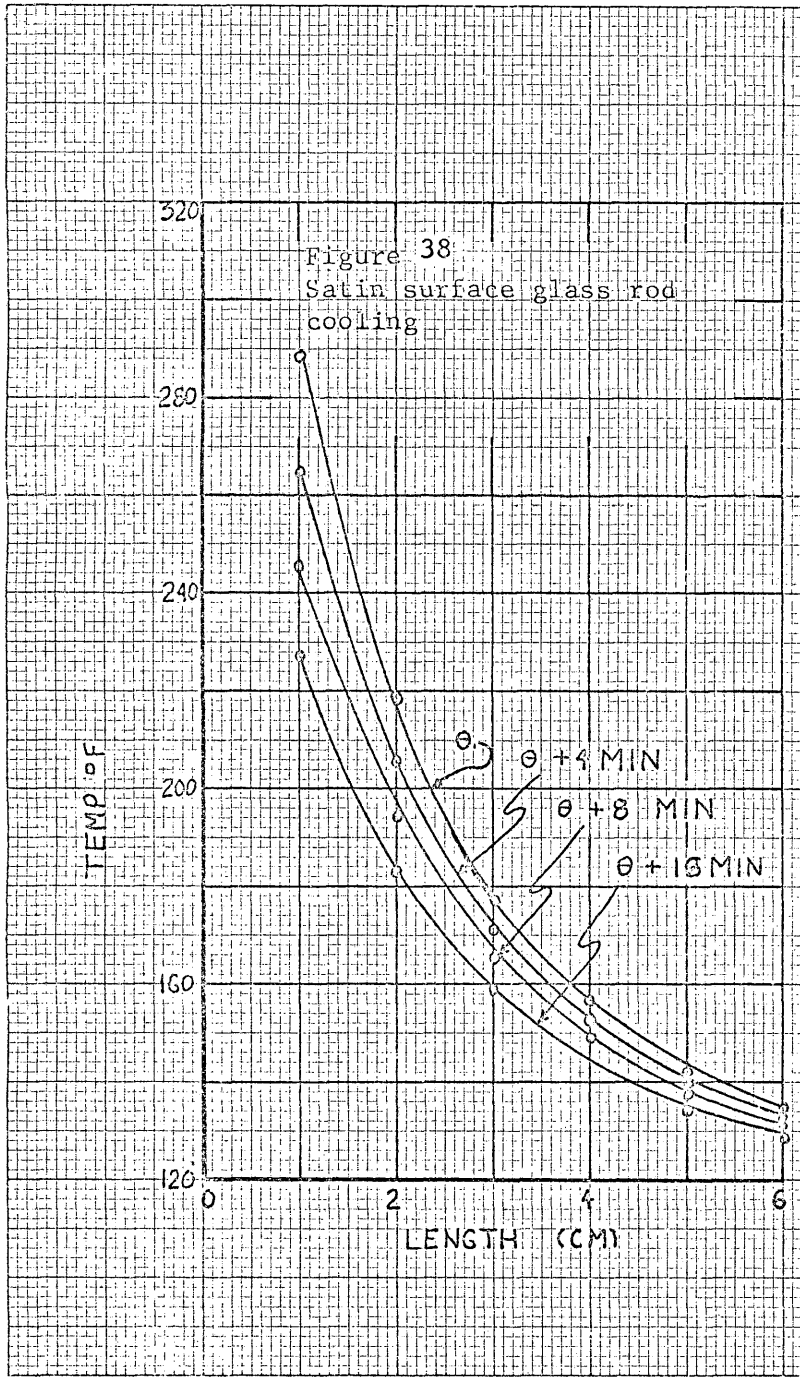

Figure 38
Satin surface glass rod
cooling

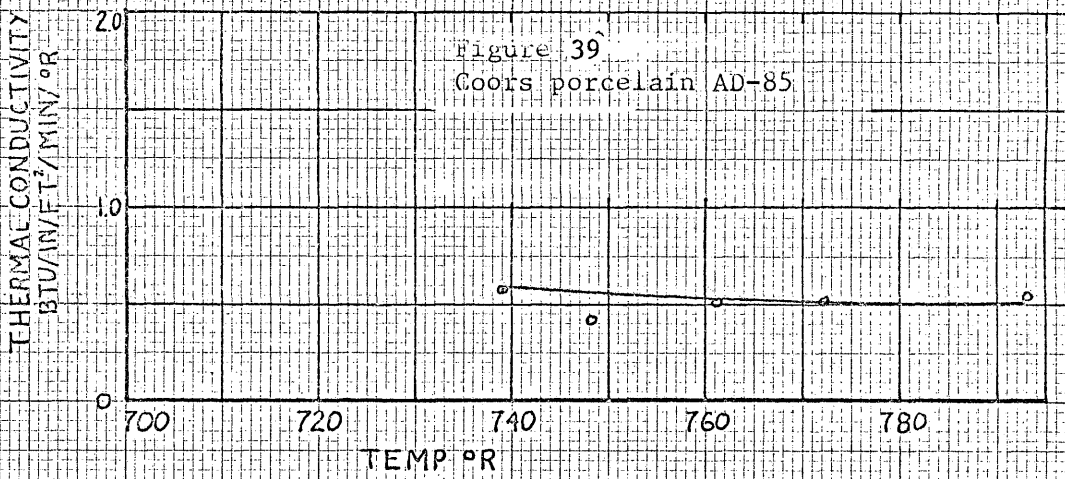

Figure 39
Coors porcelain AD-85

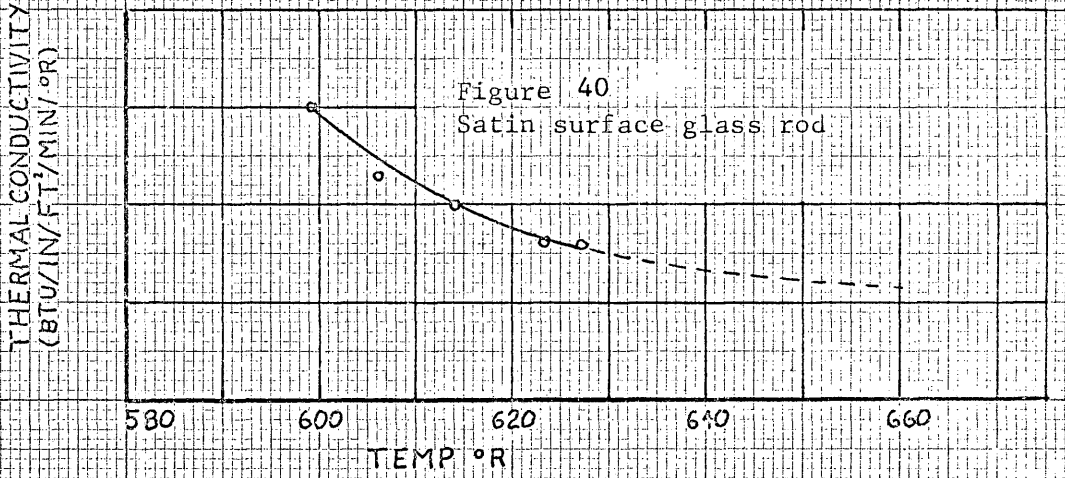

Figure 40
Satin surface glass rod

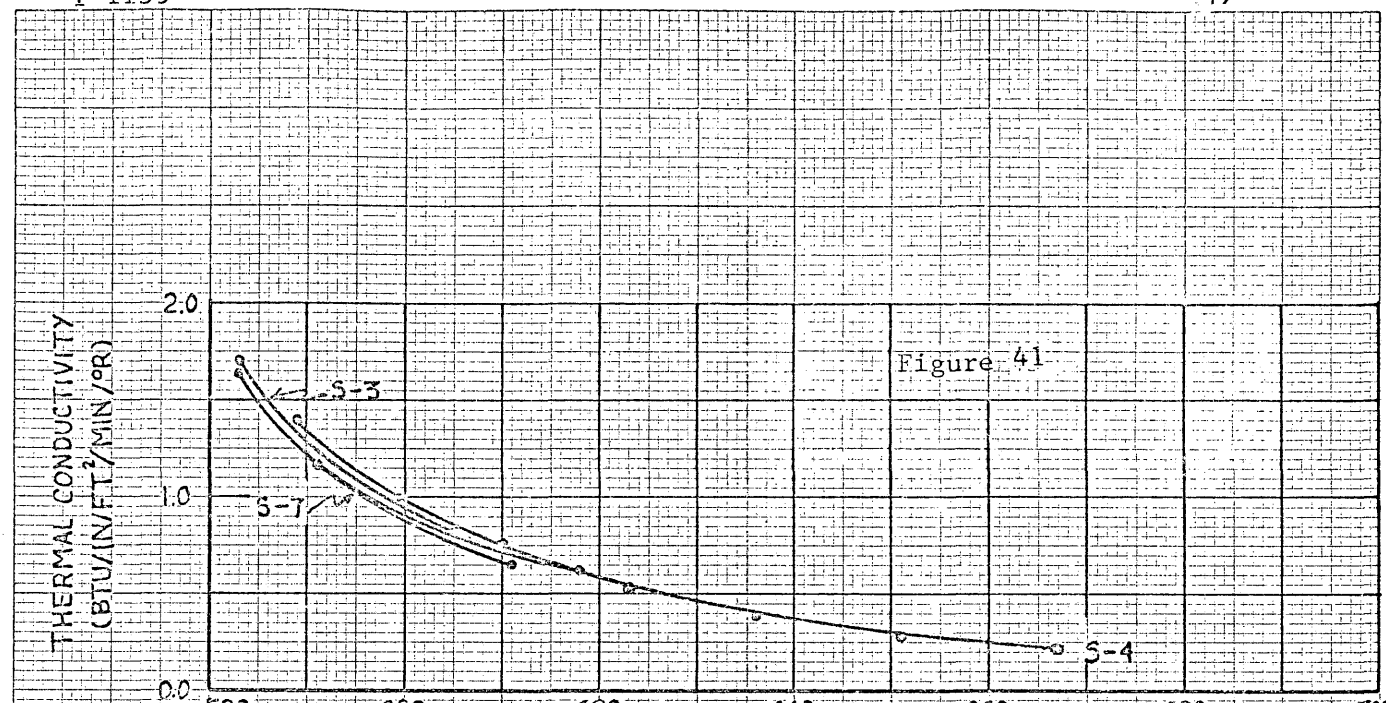

Figure 41

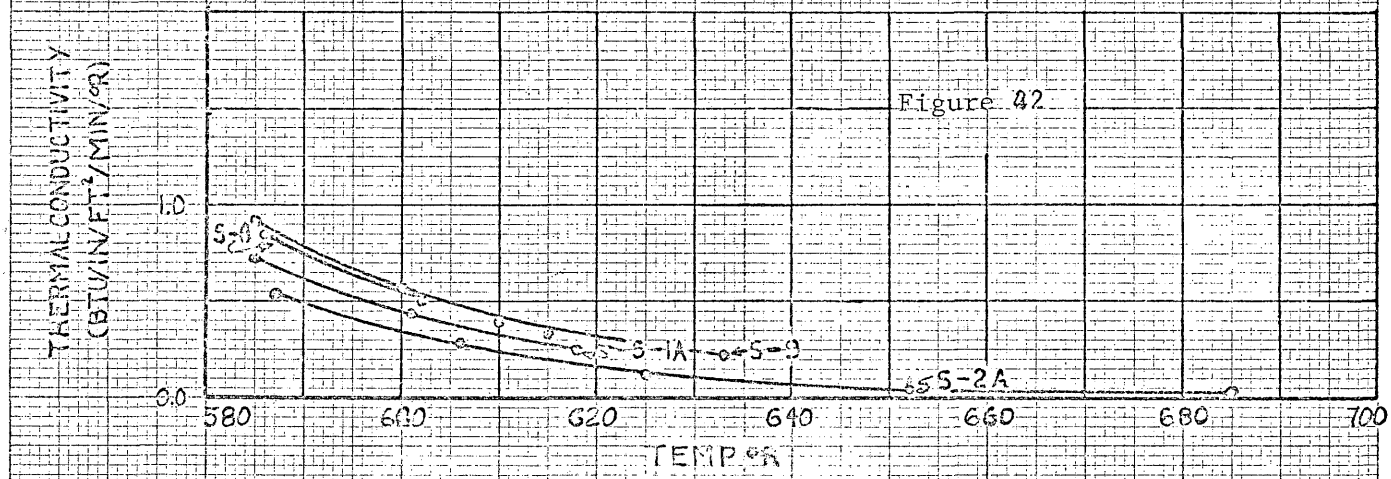

Figure 42

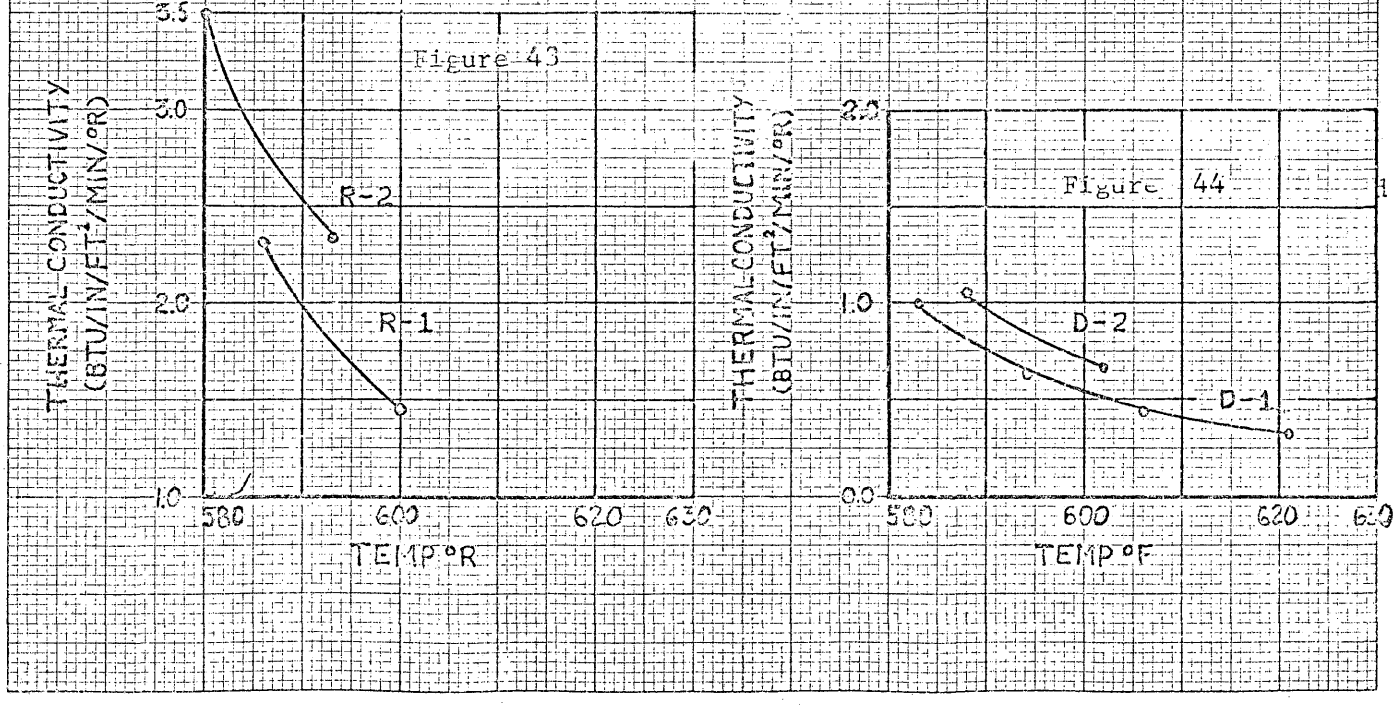

Figure 43

Figure 44

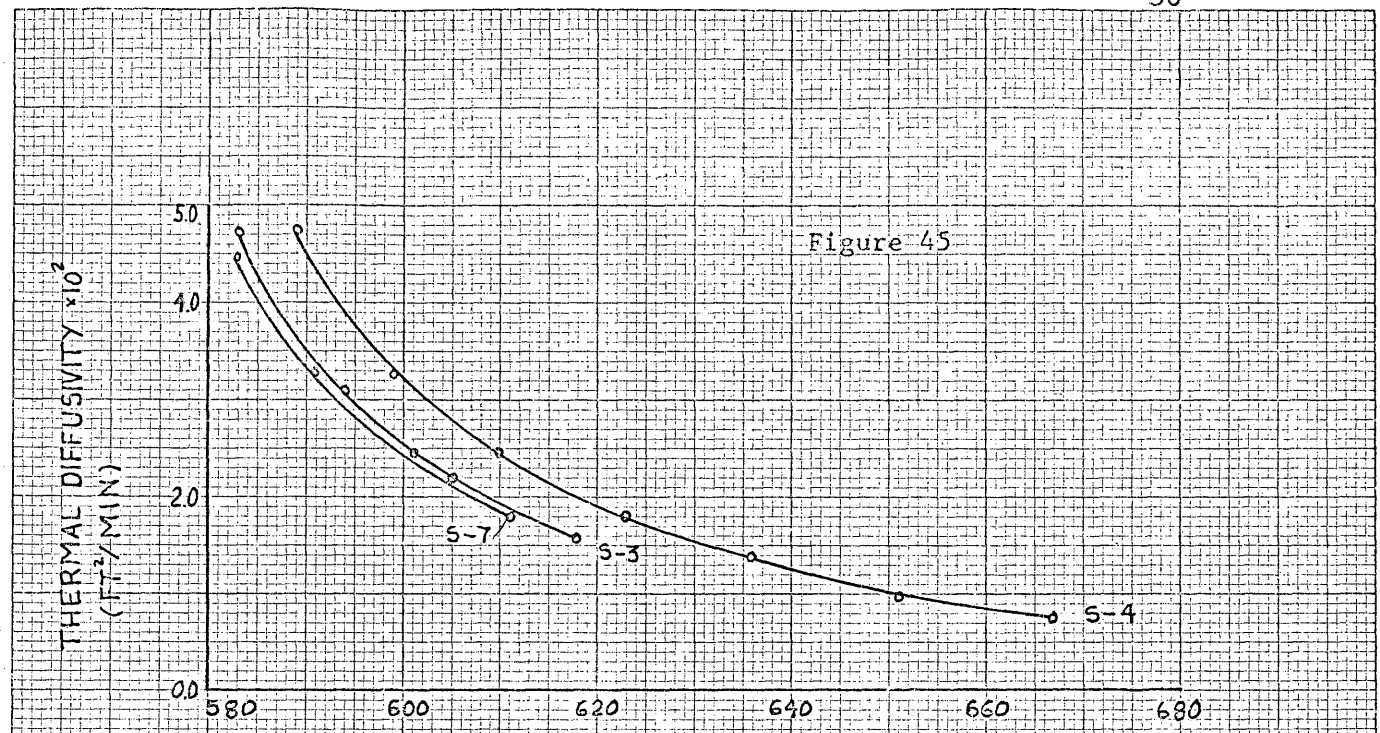

Figure 45

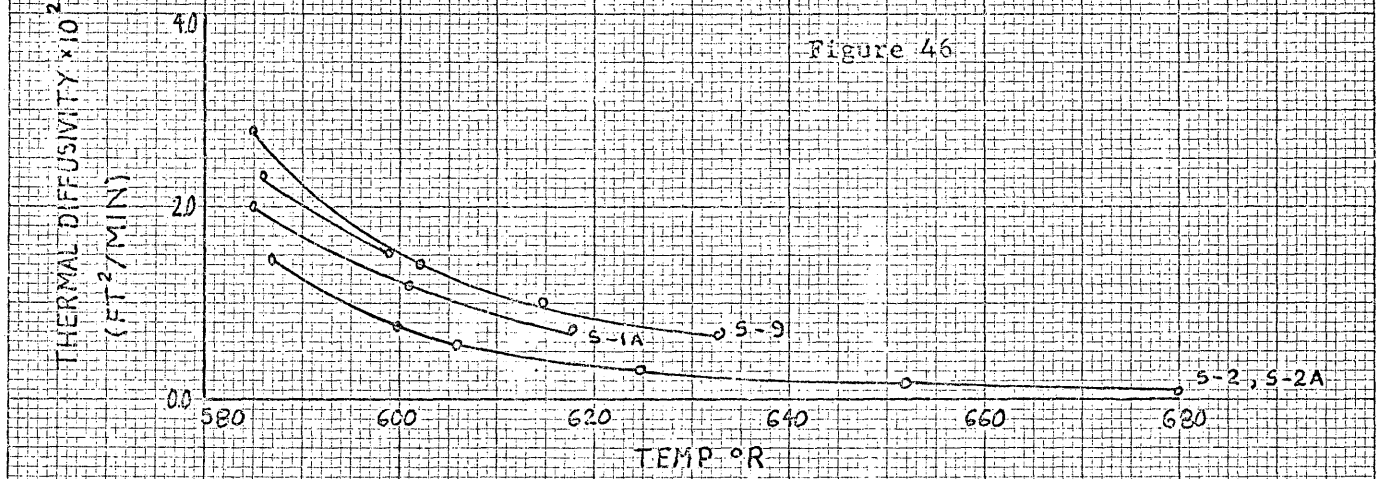

Figure 46

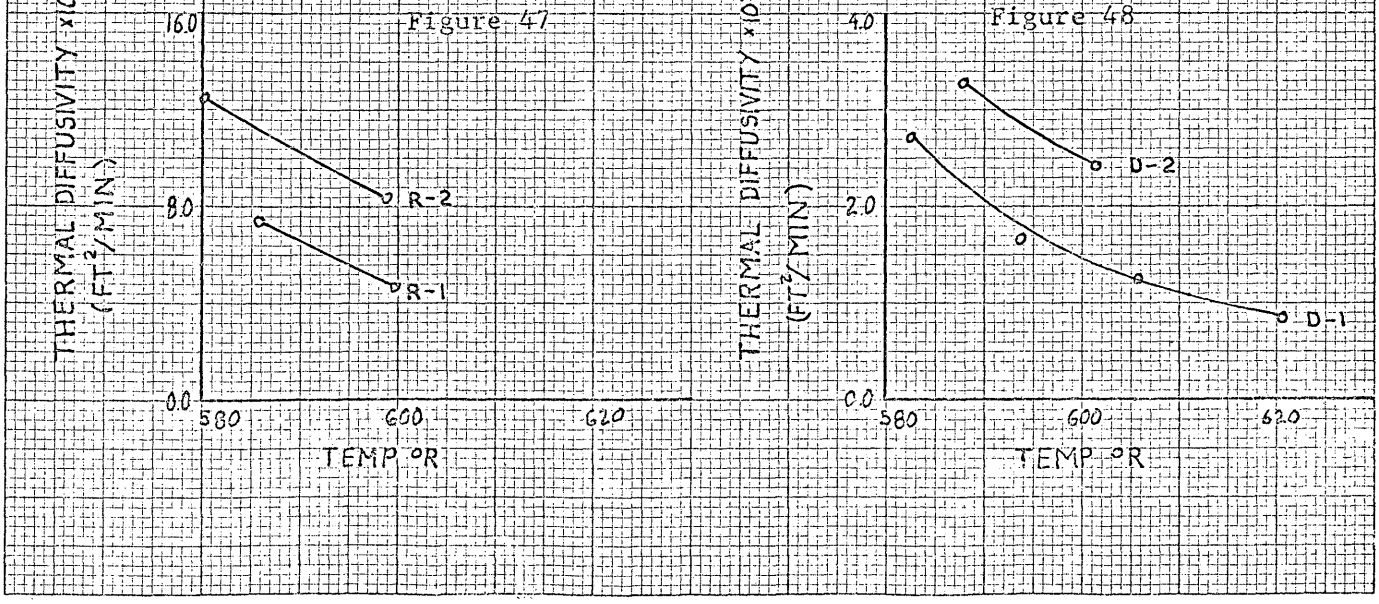

Figure 47

Figure 48

Figure 50
Temp 600°R

Figure 49
Temp 600°R

THERMAL CONDUCTIVITY
(BTU/IN/FT²/MIN/°R)
2.0
1.0
0
PERMEABILITY (md)
0
100
200
300
400
R-2
R-1
S-3
D-2
S-4
S-3
D-1
S-2
S-1A
S-7
Figure 51
Temp 540°R
THERMAL DIFFUSIVITY
(FT²/MIN)
8.0
4.0
0
PERMEABILITY (md)
0
100
200
300
400
R-2
S-3
D-2
R-1
S-4
S-3
S-1A
D-1
S-2
Figure 52
Temp 600°R

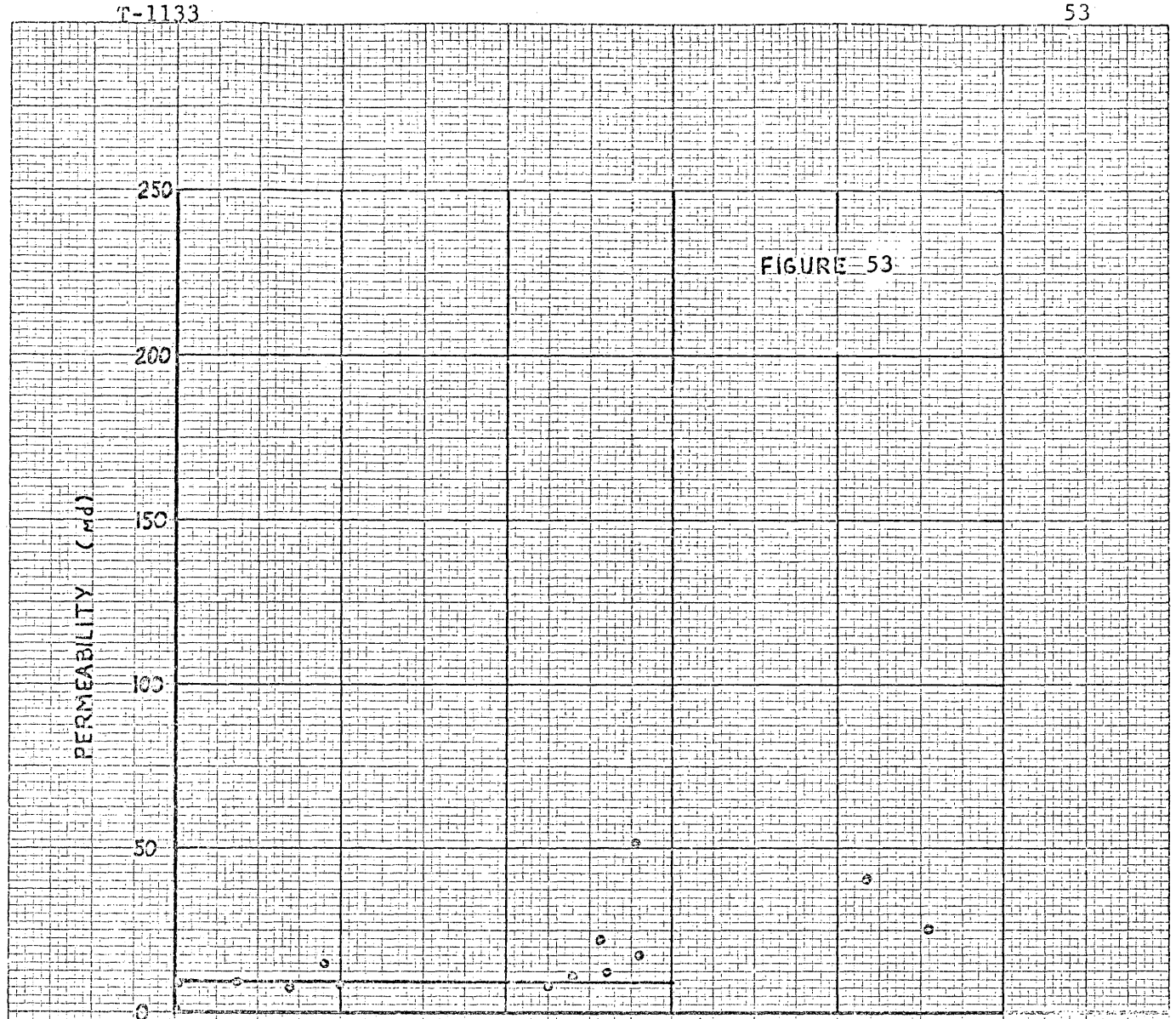

FIGURE 53

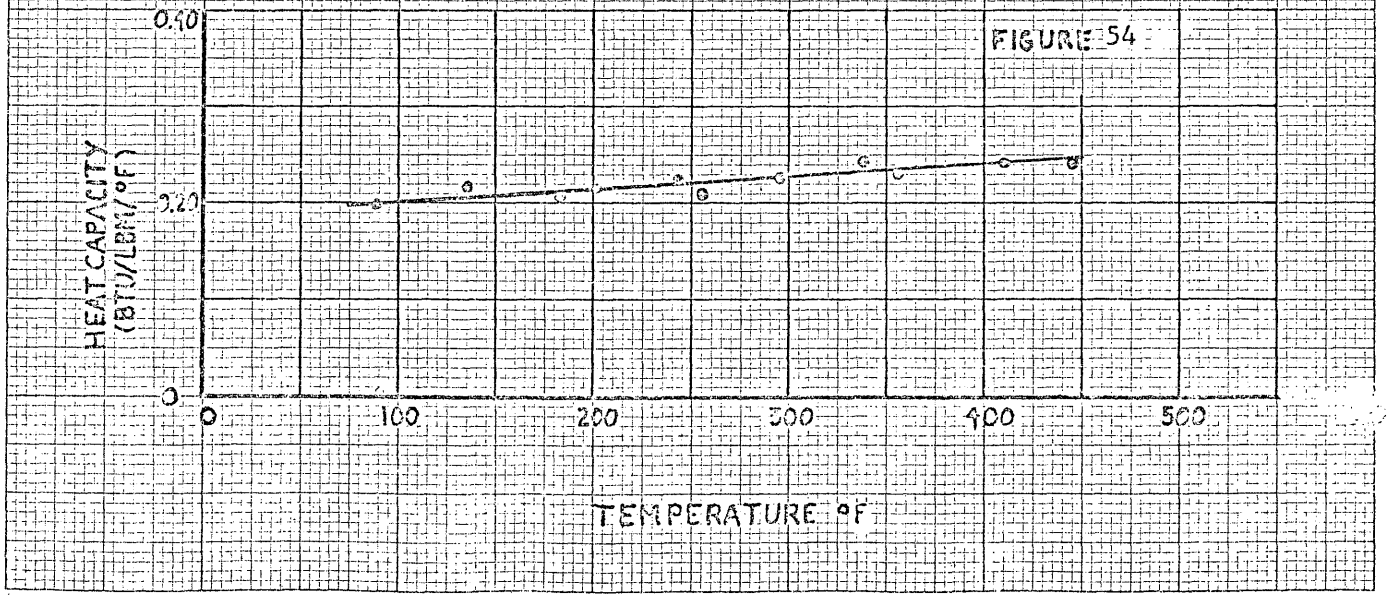

FIGURE 54

GEOLOGICAL DESCRIPTION OF SPECIMENS

Specimen	Permeability (to air)	Porosity (effective)	Description
D-1	0.2 md	9.59%	Sandstone; fine grain; well consolidated; well sorted, subangular to rounded quartz grains cemented with calcite and montmorillonite; medium gray with hornblende and mica (biotite and muscovite).
D-2	41.5 md	20.8%	Sandstone; fine to medium grain; slightly friable; well sorted, subangular to rounded quartz grains cemented with montmorillonite and calcite; medium gray with hornblende and mica.
E-1	7.57 md	7.57%	Sandstone; medium grain; slightly friable; well sorted, subangular quartz grains cemented with montmorillonite and calcite; medium gray with hornblende and mica.
E-2	3.9 md	9.82%	Same as E-1
E-3	1.9 md	7.65%	Sandstone; medium to fine grain; well consolidated; well sorted, subangular quartz grains cemented with calcite and montmorillonite; medium gray with hornblende and mica.
E-5	1.7 md	11.3%	Sandstone; fine to medium grain; well consolidated; well sorted, rounded to subangular quartz grains cemented with calcite and montmorillonite. Medium gray with hornblende and mica.

Specimen	Permeability (to air)	Porosity (effective)	Description
E-6	22.2 md	12.8%	Sandstone; medium to large grain; well consolidated; well sorted, subangular quartz grains cemented with calcite and montmorillonite; medium gray with hornblende and mica.
E-8	0.5 md	9.49%	Sandstone; fine grain; well consolidated; well sorted, subangular to rounded quartz grains cemented with calcite and montmorillonite; medium gray with hornblende and mica.
O-1	96.1 md	18.5%	Sandstone; medium to large grain; friable; well sorted, subangular quartz grains cemented with montmorillonite and calcite. Some secondary cementation with calcite and dolomite; medium gray with hornblende and mica.
R-1	25.8 md	22.7%	Sandstone; medium to fine grain; unconsolidated; well sorted, subangular quartz grains cemented with montmorillonite and calcite. Slightly laminated; medium gray with hornblende and mica. Laminating material is primarily hornblende and partially altered hornblende.
R-2	253.0 md	31.1%	Same as R-1
S-1	11.3 md	12.0%	Sandstone; medium grain; slightly friable; well sorted, subangular quartz grains cemented with montmorillonite and clacite; medium gray with horn blende and mica.

Specimen	Permeability (to air)	Porosity (effective)	Description
S-1A	11.3 md	12.0%	Same as S-1
S-2	5.0 md	8.9%	Sandstone; medium grain, friable; well sorted, subangular quartz grains cemented with montmorillonite and calcite; medium gray with hornblende and mica.
S-2A	5.0 md	8.9%	Same as S-2
S-3	12.5 md	13.0%	Sandstone; medium grain; well consolidated well sorted, subangular quartz grains cemented with calcite and montmorillonite; medium gray with hornblende and mica.
S-4	15.0 md	14.1%	Sandstone; medium grain; well consolidated; well sorted, subangular to rounded quartz grains cemented with montmorillonite and calcite; medium gray with hornblende and mica.
S-5A	7.0 md	10.8%	Same as S-5
S-6	82.6 md	14.5%	Sandstone; medium to fine grain; slightly friable; well sorted, subangular quartz grains cemented with montmorillonite and calcite; medium gray with hornblende and mica.
S-7	0.1 md	11%	Sandstone; fine to medium grain; well consolidated; well sorted, subangular quartz grains cemented with calcite and montmorillonite; medium gray with hornblende and mica.

Specimen	Permeability (to air)	Porosity (effective)	Description
S-8	52.6 md	13.9%	Sandstone; medium grain; slightly consolidated; well sorted, subangular quartz grains cemented with montmorillonite; medium gray with hornblende and mica.
S-9	4.5 md	14.6%	Sandstone; fine grain; well consolidated; well sorted, rounded to subangular quartz grains cemented with calcite and montmorillonite; medium gray with hornblende and mica.
S-10	2.7 md	12.8%	Sandstone; medium to fine grain well consolidated; well sorted, subangular quartz grains cemented with calcite and montmorillonite; medium gray with nornblende and mica.
S-11	0.2 md	5.5%	Sandstone; fine grain; well consolidated; well sorted, subangular to rounded quartz grains cemented with calcite and clay; medium gray with hornblende and mica.

TABLE 2

STEADY-STATE TEMPERATURE EQUATIONS AND DERIVATIVE AS A FUNCTION OF LENGTH

Specimen	Current Input (Amps)	Equation and Derivitive
D-1	1.0	$T = 186.0 - 28.84X + 2.36X^2$ $dt/dx = -28.84 + 4.72X$
	2.0	$T = 395.4 - 88.39X + 8.28X^2$ $dt/dx = -88.39 + 16.56X$
D-2	1.0	$T = 165.4 - 27.01X + 1.9X^2$ $dt/dx = -27.01 + 3.8X$
	2.0	$T = 297.7 - 57.7X + 3.85X^2$ $dt/dx = -57.7 + 7.7X$
E-1	1.0	$T = 175.0 - 27.26X + 2.14X^2$ $dt/dx = -27.26 + 4.28X$
	3.0	$T = 563.4 - 210.3X + 24.9X^2$ $dt/dx = -210.3 + 49.8X$
E-2	1.0	$T = 183.4 - 30.69X + 2.29X^2$ $dt/dx = -30.69 + 4.58X$
	2.0	$T = 401.0 - 96.78X + 8.8X^2$ $dt/dx = -97.78 + 16.2X$
E-3	1.0	$T = 205.0 - 39.29X + 3.23X^2$ $dt/dx = -39.29 + 6.46X$
	2.0	$T = 437.2 - 106.6X + 8.7X^2$ $dt/dx = -106.6 + 17.4X$
	3.0	$T = 624.5 - 159.4X + 13.2X^2$ $dt/dx = -159.4 + 26.4X$

TABLE 2 (Continued)

Specimen	Current Input (Amps)	Equations and Derivative
E-5	1.0	$T = 184.86 - 24.88X + 1.55X^2$ $dt/dx = -24.88 + 3.1X$
	2.0	$T = 419.0 - 90.92X + 7.08X^2$ $dt/dx = -90.92 + 14.16X$
	3.0	$T = 624.3 - 136.5X + 10.5X^2$ $dt/dx = -136.5 + 21.0X$
E-6	1.0	$T = 182.06 - 26.06X + 2.07X^2$ $dt/dx = -26.06 + 4.14X$
E-8	1.0	$T = 161.6 - 20.17 + 1.28X^2$ $dt/dx = -20.17 + 2.56X$
	2.0	$T = 365.86 - 68.59X + 4.98X^2$ $dt/dx = -68.59 + 9.96X$
	3.0	$T = 530.7 - 114.4X + 8.9X^2$ $dt/dx = -114.4 + 17.8X$
O-1	1.0	$T = 129.8 - 11.76X + .6X^2$ $dt/dx = -11.76 + 1.2X$
	2.0	$T = 305.8 - 58.47X + 3.9X^2$ $dt/dx = -58.47 + 7.8X$
	3.0	$T = 460.7 - 104.36X + 8.1X^2$ $dt/dx = -104.36 + 16.2X$
R-1	1.0	$T = 165.4 - 28.45X + 2.29X^2$ $dt/dx = -28.45 + 4.58X$
	2.0	$T = 429.3 - 190.0X + 40.87X^2$ $dt/dx = -190.0 + 82.7X$
R-2	1.0	$T = 151.7 - 24.11X + 1.95X^2$ $dt/dx = -24.11 + 3.9X$

TABLE 2 (Continued)

Specimen	Current Input (Amps)	Equations and Derivative
	2.0	$T = 352.1 - 92.9X + 8.7X^2$ $dt/dx = - 92.9 + 17.4X$
S-1	1.0	$T = 291.2 - 78.7X + 8.36X^2$ $dt/dx = - 78.7 + 16.72X$
	2.0	$T = 403.4 - 107.1X + 10.75X^2$ $dt/dx = - 107.1 + 21.5X$
S-1A	1.0	$T = 188.9 - 35.38X + 3.02X^2$ $dt/dx = - 35.38 + 6.04X$
	2.0	$T = 365.1 - 83.9X + 7.45X^2$ $dt/dx = - 83.9 + 14.9X$
S-2A	1.0	$T = 178.6 - 38.3X + 3.7X^2$ $dt/dx = - 38.3 + 7.4X$
	2.0	$T = 327.6 - 74.8X + 6.04X^2$ $dt/dx = - 74.8 + 6.04X$
	3.0	$T = 450.0 - 105.8X + 8.5X^2$ $dt/dx = - 105.8 + 17.0X$
S-3	1.0	$T = 179.2 - 23.6X + 1.43X^2$ $dt/dx = - 23.6 + 2.76X$
	2.0	$T = 315.0 - 58.8X + 3.97X^2$ $dt/dx = - 58.8 + 7.94X$
	3.0	$T = 479.7 - 94.1X + 6.4X^2$ $dt/dx = - 94.1 + 12.8X$
S-4	1.0	$T = 232.6 - 28.4X + 1.4X^2$ $dt/dx = - 28.4 + 2.8X$
S-5	1.0	$T = 146.5 - 19.5X + 1.3X^2$ $dt/dx = - 19.5 + 2.6X$

TABLE 2 (Continued)

Specimen	Current Input (Amps)	Equations and Derivative
	2.0	$T = 305.6 - 61.6X + 4.5X^2$ $dt/dx = - 61.6 + 9.0X$
S-6	1.0	$T = 147.7 - 19.7X + 1.4X^2$ $dt/dx = - 61.6 + 9.0X$
S-	2.0	$T = 260.6 - 43.1X + 2.6X^2$ $dt/dx = - 43.1 + 5.2X$
	3.0	$T = 299.7 - 51.1X + 3.1X^2$ $dt/dx = - 51.1 + 6.2X$
S-7	1.0	$T = 169.0 - 20.2X + 1.44X^2$ $dt/dx = - 20.2 + 2.88X$
	3.0	$T = 379.2 - 72.4X + 5.8X^2$ $dt/dx = - 72.4 + 11.6X$
S-8	1.0	$T = 168.8 - 31.1X + 2.6X^2$ $dt/dx = - 31.1 + 5.2X$
	2.0	$T = 298.4 - 56.6X + 3.8X^2$ $dt/dx = - 56.6 + 7.6X$
	3.0	$T = 440.8 - 87.1X + 5.9X^2$ $dt/dx = - 87.1 + 11.8X$
S-9	1.0	$T = 204.0 - 35.1X + 2.6X^2$ $dt.dx = - 35.1 + 5.2X$
	2.0	$T = 416.0 - 90.4X + 7.2X^2$ $dt/dx = - 90.4 + 14.4X$
	3.0	$T = 592.3 - 139.1X + 11.3X^2$ $dt/dx = - 139.1 + 22.6X$
S-10	1.0	$T = 138.8 - 13.6X + .7X^2$ $dt/dx = - 13.6 + 1.4X$
	2.0	$T = 312.0 - 50.7X + 3.1X^2$ $dt/dx = - 50.7 + 6.2X$

TABLE 2 (Continued)

Specimen	Current Input (Amps)	Equation and Derivative
	3.0	$T = 449.5 - 74.2X + 4.4X^2$ $dt/dx = - 74.2 + 8.8X$
S-11	1.0	$T = 196.0 - 12.7X + .75X^2$ $dt/dx = - 12.7 + 1.5X$
	2.0	$T = 399.0 - 87.3X + 8.8X^2$ $dt/dx = - 87.3 + 17.6X$
	3.0	$T = 670.7$ 0 $185.3X + 21.2X^2$ $dt/dx = - 185.3 + 42.4X$

TABLE 2A

STEADY-STATE AND COOLING EQUATIONS
PERTAINING TO STANDARD MATERIALS
Coors Porcelain AD-85

Length	Equation	Remarks
10.0 cm	$T = 234.2 - 10.6X + .43X^2$ $dt/dx = - 10.6 + .86X$	Steady State
"	$T = 366.9 - 16.9X + .8X^2$ $dt/dx = - 16.9 + 1.6X$	Cooling, θ_1
"	$T = 339.1 - 12.5X + .6X^2$ $dt/dx = - 12.5 + 1.2X$	Cooling, θ_1 + 2 min
8.0 cm	$T = 281.1 - 16.4X + 1.X^2$ $dt/dx = - 16.4 + 2.X$	Steady State
"	$T = 253.0 - 4.6X + .1X^2$ $dt/dx = - 4.6 + .2X$	Cooling, θ_1
"	$T = 241.0 - 2.75X + .1X^2$ $dt/dx = - 2.75 + .2X$	Cooling, θ_1 + 1.5 min
6.0 cm	$T = 216.6 - 6.5X + .12 X^2$ $dt/dx = - 6.5 + .24X$	Heating, θ = 24 min
"	$T = 244.5 - 7.5X$	Heating, θ = 36 min
"	$T = 256.9 - 5.5X + .4X^2$	Heating, θ = 52 min

TABLE 2A (Continued)

SATIN SURFACE QUARTZ ROD

Length	Equation	Remarks
10 cm	$T = 444.6 - 70.4X + 3.8X^2$ $dt/dx = - 70.4 + 7.6X$	Steady State
"	$T = 229.4 - 24.23X + 1.24X^2$ $dt/dx = - 24.23 + 2.48X$	Cooling, θ_1
"	$T = 201.4 - 17.2X + .8X^2$ $dt/dx = - 17.2 + 1.6X$	Cooling, θ_1 + 5 min
"	$T = 180.25 - 12.8X + .6X^2$	Cooling, θ_1 + 9 min
8 cm	$T = 311.6 - 87.2X + 9.4X^2$ $dt/dx = - 87.2 + 18.8X$	Steady State
6 cm	$T = 277.0 - 39.5X + 2.7X^2$ $dt/dx = - 39.5 + 5.4X$	Steady State

COOLING CURVE EQUATIONS FOR SPECIMEN S-1

Time	Equation
θ_1	$T = 355.5 - 79.7X + 7.3X^2$ $dt/dx = - 79.7 + 14.6X$
θ_1 + 4 min	$T = 320.7 - 65.9X + 5.8X^2$ $dt/dx = - 65.9 + 11.6X$
θ_1 + 8 min	$T = 294.0 - 57.9X + 5.3X^2$ $dt/dx = - 57.9 + 10.6X$
θ_1 + 12 min	$T = 265.6 - 46.5X + 4.0X^2$ $dt/dx = - 46.5 + 8.0X$

TABLE 3

PHYSICAL AND THERMAL PROPERTIES OF SPECIMENS

Specimen	Porosity %	Permeability md	Density lb/ft^3	Temperature ^{o}R	Thermal Conductivity	Thermal Diffusivity
D-1	9.6	0.2	150.07	621	.316	$.85 \times 10^{-2}$
				606	.460	1.23×10^{-2}
				594	.617	1.65×10^{-2}
				583	1.010	1.70×10^{-2}
D-2	20.9	41.5	131.5	602	.670	2.4×10^{-2}
				588	1.06	3.22×10^{-2}
E-1	7.57	3.5	153.4	611	.384	1.04×10^{-2}
				597	.672	1.76×10^{-2}
				585	1.01	2.63×10^{-2}
E-2	9.82	1.9	149.8	617	.366	$.98 \times 10^{-2}$
				601	.568	1.50×10^{-2}
				587	.920	1.46×10^{-2}
E-5	11.3	1.7	147.2	623	.465	1.27×10^{-2}

TABLE 3 (Continued)

Specimen	Porosity %	Permeability md	Density lb/ft^3	Temperature ^oR	Thermal Conductivity	Thermal Diffusivity
E-5 (Continued)				609	.650	1.178×10^{-2}
				597	.920	1.58×10^{-2}
				586	1.36	3.714×10^{-2}
E-6	12.8	22.2	144.7	619	.375	1.0×10^{-2}
				606	.532	1.47×10^{-2}
				595	.757	2.10×10^{-2}
R-1	22.7	25.8	128.3	600	1.45	4.55×10^{-2}
				586	2.33	7.29×10^{-2}
R-2	31.7	253.0	114.4	591	2.34	8.20×10^{-2}
				578	3.70	12.90×10^{-2}
S-1A	12.0	11.3	146.0	618	.257	$.71 \times 10^{-2}$
				601	.432	1.18×10^{-2}
				585	.720	1.98×10^{-2}
S-2	8.9	5.0	151.2	723	0.031	0.82×10^{-3}
				685	0.036	0.96×10^{-3}

TABLE 3 (Continued)

Specimen	Porosity %	Permeability md	Density lb/ft^3	Temperature ^{o}R	Thermal Conductivity	Thermal Diffusivity
				652	0.0615	1.63×10^{-3}
				625	0.113	3.00×10^{-3}
S-2A	8.9	5.0	151.2	606	0.216	5.73×10^{-3}
				600	0.296	7.86×10^{-3}
				587	0.542	14.3×10^{-3}
S-3	13.0	12.5	144.4	618	0.545	1.52×10^{-2}
				605	0.780	2.17×10^{-2}
				594	1.100	3.06×10^{-2}
				583	1.690	4.70×10^{-2}
S-4	14.1	15.0		667	0.220	$.74 \times 10^{-2}$
				651	0.270	
				636	0.382	
				623	0.528	
				610	.72	
				599	.967	

TABLE 3 (Continued)

Specimen	Porosity %	Permeability md	Density lb/ft^3	Temperature ^{o}R	Thermal Conductivity	Thermal Diffusivity
S-4 (Continued)				589	1.39	
S-6	14.5	82.6	141.9	590	1.26	3.57×10^{-2}
				580	1.86	5.25×10^{-2}
S-7	11.0	0.1	147.7	611	.66	1.79×10^{-2}
				601	.894	2.43×10^{-2}
				591	1.19	3.24×10^{-2}
				583	1.64	4.464×10^{-2}
S-8	13.9	52.6	146.2	602	.50	1.38×10^{-2}
				586	.83	2.284×10^{-2}
S-9	14.6	4.5	135.8	633	.227	$.67 \times 10^{-2}$
				615	.338	1.00×10^{-2}
				599	.538	1.50×10^{-2}
				585	.886	2.75×10^{-2}

IBM OS/360 BASIC FORTRAN IV(E) COMPILATION

```
  3   FORMAT (3F10.4)
  4   FORMAT (12)
  5   FORMAT (215)
 10   READ (1, 4)  IP
      IF (IP-99)  11, 12, 12
 11   READ (1, 5)  N, NP
      READ (1, 3)  (C1, C2, C3, 1=1, N)
      CALL FIT (NP, C1, C2, C3, N)
      GO TO 10
 12   STOP
      END
```

END OF COMPILATION MAIN

IBM OS/360 BASIC FORTRAN IV(E) COMPILATION

```
      SUBROUTINE FIT (IP, C1, C2, C3, N)
C     THIS SUBROUTINE CALCULATED THE RADIATION-CONDUCTION
      RATIO (D/k=RCTA) DOUBLE PRECISION T1(20), TA (20),
      TAA (20), TSA
      DIMENSION DT1 (20), DT2 (20), RCTA (20)
      WRITE (3, 3)
  3   FORMAT ('1')
      D=1.0
      TS=565.0
      DX=0.25
      ACS=(3.14*(D**2.0))/(4.0*144.0)
      AR=3.14*D*DX/144.0
      X1=.25
      DO 1 I=1,IP
      X2=X1+DX
      A=X1*2.54
      B=X2*2.54
      T1(I)=C1+C2*A+C3*A**2.
      T2(I)=C1+C2*B+C3*B**2.
      DT1(I)=(C2+2*C3*A)*2.54
      DT2(I)=(C2+2*C3*B)*2.54
```

```
      TA(I)=((T1(I)/T2(I))/2.)/460
      TSA=ts**4.0
      TAA(I)=(((T1(I)/460.0)**4.0/(T2(I)/460.0)**4.0)/2.)**0.25
      C=ACS*(DT2(I)-DT1(I))
      F=2.856E-11*AR*(TAA(I)**4.0-TSA)
      RCTA(I)-C/F
      TA(I)=TA(I)-460.
      X1=X2
      WRITE (3, 2) TA(I), RCTA(I), DT1(I), DT2(I), TAA(I)
1     CONTINUE
2     FORMAT (5X, 4HTAVG, F7.2, 2X, 4HRCTA, 2X, 1HK, E20.8,
             3F10.5)
      RETURN
      END
```

END OF COMPILATION FIT

IBM OS/360 BASIC FORTRAN IV(E) COMPILATION

```
      PROGRAM II
C     THERMAL CONDUCTIVITY COEFE CALCULATIONS
C     T1 IS TEMP AT X1 FOR STEADY STATE CONDITIONS
C     T2 IS SAME AS T1 BUT FOR X2
C     T1D IS THE DERIVATIVE OF T1 AT X1
C     T2D IS SAME AS T1D BUT AT X2
C     F(TAAC) IS D/k=F(TAA) FROM STEADY STATE CURVE
C     A IS TAA BETWEEN X1 AND X2 FOR TIME 1
C     B IS SAME AS A BUT FOR TIME 2
C     TAAC IS RADIATION SURFACE TEMPERATURE
C     TA1 IS AVE TEMP BETWEEN X1 AND X2 AT TIME 1
C     TA2 IS AVE TEMP BETWEEN X1 AND X2 AT TIME 2
      DOUBLE PRECISION A, XKD, B, TS, TA1, XK, ADV
      DOUBLE PRECISION TA2, XKN, TAAC
      DIMENSION HEAD (20)
      T1(X)=C1/C2*X/C3*X*X/C4*X**3./C5*X**4./460.
      T2(X)=D1/D2*X/D3*X*X/D4*X**3./D5*X**4./460.
      T1D(X)=(C2/2.*C3*X/3.*C4*X*X/4.*C5*X**3.)*2.54
      T2D(X)=(D2/2.*D3*X/3.*D4*X*X/4.*D5*X**3.)*2.54
      F(TAAC)=F1/F2*TAAC/F3*TAAC**2/F4*TAAC**3
      DX=0.25*2.54
      TS-565
      READ(1, 2) HEAD
```

```
    1   FORMAT (3F5.0,12,F10.0)
        DEN=DEN*2.54
        READ (1, 3) F1, F2, F3, F4
    3   FORMAT (3F10.4)
        WRITE (3, 4) HEAD
    4   FORMAT ('0', 20A4)
        WRITE (3, 5) XMASS, CP, DZ
    5   FORMAT ('MASS=', F5.4, 2X, 'CP=', F4.3, 'DZ-', F4.2)
        N=N-1
        READ (1, 7) TH1, C1, C2, C3, C4, C5
        DO 30 I=1, N
        WRITE (3,200)
  200   FORMAT (//)
        READ (1, 7) TH2, D1, D2, D3, D4, D5
    7   FORMAT (6F10.0)
        XL=
  100   XL=XL/DX
        IF9DEN-XL) 6, 8, 8
    8   A=((T1(XL)**4/T1(XL/DX)**4)/2.)**0.25
        B=((T2(XL)**4/T2(XL/DX)**4)/2.)**0.25
        TAAC=((A**4./B**4.)/2.)**.25
        TA1=(T1(XL)/T1(XL/DX00/2.
        TA2=(T2(XL)/T@(XL/DX))/2.
        XKN=XMASS*CP*(TA2-TA1)/(TH2-TH1)
        XKD=((T1D(XL/DX)/T2D(XL/DX))/2.-(T1D(XL)/T2D(XL))/2.*5.45E-
        1-F(TAAC)*2.856E-11*.00545*(TAAC**4-TS**4
        XK=XKD
        ADV=(Ta1/Ta2)/2.
        WRITE(93, 20) XK, ADV, XL
   20   FORMAT (3E20.8)
        GO TO 100
    6   C1=D1
        C2=D2
        C3=D3
        C4=D4
        C5=D5
        TH1=TH2
   30   CONTINUE
        STOP
        END
```

END OF COMPILATION MAIN

SELECTED BIBLIOGRAPHY

1. Bailey, N. P., 1931, Response of thermocouples: Mechanical Engineer, V. 53, n. 11, p. 797.

2. Bailey, M. P., 1932, The measurement of surface temperatures: Mechanical Engineer, V. 54, n. 8, p. 553.

3. Birch, F., and Clark, H., 1940, The Thermal conductivities of rocks and its dependence upon temperature and composition: American Journal of Science, V. 238, p. 529.

4. Carslaw, H. S., and Jaeger, J. C., 1959, Conduction of heat in solids: 2nd ed., London, Oxford University Press.

5. Compton, Arthur H., 1915, The variation of the specific heat of solids with temperature: The Physical Review, V. 6, 2nd series, p. 377-389.

6. Compton, A. H., 1916, A physical study of the thermal conductivities of solids: The Physical Review, V. 7, 2nd series series, p. 341-348.

7. Compton, A. H., 1916, On the location of thermal energy of solids: The Physical Review, V. 7, 2nd series, p. 349-355.

8. Green, A. T., 1926-1927, Comparison of thermal diffusivities and conductivities of silica and fire clay refractories: Trans. Ceram.

9. Ingersoll, L. R., and Koepp, O. A., 1924, Thermal diffusivity and conductivity of some soil materials: The Physical Review, V. 24, p. 92-93.

10. Ingersoll, L. R., and Zobel, O. J., 1948, Heat conduction: 1st ed., New York, McGraw-Hill Book Company.

11. Jakob, M., 1949, Heat Transfer: 2 vols., New York, John Wiley & Sons, Inc.

BIBLIOGRAPHY (Continued)

12. King, R. W., 1915, A method of measuring heat conductivities: The Physical Review, V. 6, n. 6, p. 437-445.

13. Kingery, W. D., 1954, Thermal conductivity, VI, Determination of conductivity of Al_2O_3 by spherical envelope and cylinder methods: American Ceramic Society Journal, V. 37, p. 88.

14. Kreith, Frank, 1958, Principles of heat transfer: 2nd ed., Scranton, Pennsylvania, International Text Book Company.

15. Kunii, D., and Smith, J. M., 1960, Heat transfer characteristics of porous rocks.

16. Kunii, D., and Smith, J. M. 1961, Thermal conductivity of porous rocks filled with stagnant fluid: Trans. AIME., V. 222, p. 37.

17. McQuarrie, M., 1954, Analysis of variation of conductivity with temperature: Journal of American Ceramic Society, V. 37, n. 2, p. 91.

18. Roeser, E., 1931, The passage of gas through walls of pyrometer protection tubes at high temperatures: Journal of the Bureau of Standards, V. 7, n. 9, p. 485.

19. Schotte, William, 1960, Thermal conductivity of packed beds: A. I. Ch. E Journal, V. 6, n. 1, p. 63.

20. Schneider, P. J., 1955, Conduction heat transfer: Reading, Massachusetts, Addison Wesley Publishing Company.

21. Somerton, W. H., 1958, Some thermal characteristics of porous rocks: Trans. AIME, V. 213, p. 375.

22. Somerton, W. H., and Boozer, G. D., 1960, Thermal characteristics of porous rock at elevated temperatures: Trans. AIME, V. 219, p. 418.

BIBLIOGRAPHY (Continued)

23. Starr, C., 1937, An improved method for the determination of thermal diffusivities: Review of Scientific Instruments, V. 8, p. 61-64.

24. Thwing, Charles B., 1906, Measurements of internal temperature: The Physical Review, V. 23, p. 315-320.

25. Weber, R. L., 1950, Heat and temperature measurement: New York, Prentice-Hall, Inc.

26. Zierfuss, H., and van der Vliet, G., 1956, Laboratory measurements of heat conductivity of sedimentary rocks: AAPG, V. 40, p. 2475.